

## Supporting Information for

### **Unveiling the Roles of Aromaticity on Optoelectronic and Charge-Transport Properties of Dehydrobenzo[*n*]annulenes**

Yu Lin,<sup>a#</sup> Yu Ge,<sup>b#</sup> Chaojie Xu,<sup>a#</sup> Haiming Zhang,<sup>a</sup> Chaohua Cui,<sup>b</sup> Yue Wu,<sup>\*b</sup> Lifeng Chi<sup>\*a</sup> and Qiang Chen<sup>\*a</sup>

<sup>a</sup> State Key Laboratory of Bioinspired Interfacial Materials Science, Institute of Functional Nano & Soft Materials (FUNSOM), Soochow University, Suzhou 215123, P. R. China

<sup>b</sup> Laboratory of Advanced Optoelectronic Materials, Key Laboratory of Novel Semiconductor-Optoelectronics Materials and Devices, College of Chemistry Chemical Engineering and Materials Science, Soochow University, Suzhou, 215123 P. R. China

<sup>#</sup> These authors contributed equally to this work.

### **Table of Contents**

General Methods .....	S2
Synthetic Procedures.....	S3
X-ray Single Crystal Structures .....	S9
DFT Calculations .....	S14
UV-vis Absorption Spectra .....	S16
Hole Mobility Measurements .....	S17
X-ray Diffraction Patterns of Thin Films.....	S18
Thermal Analysis .....	S19
NMR Spectra .....	S21
MALDI-TOF MS Spectra.....	S30
References.....	S32
Calculated Molecular Cartesian Coordinates.....	S33

## General Methods

Unless otherwise mentioned, all reactions were conducted in oven-dried glassware under an argon atmosphere using standard Schlenk techniques. All commercially available solvents and reagents were employed directly as received. Thin layer chromatography (TLC) was done on silica gel coated aluminum sheets with F254 indicator and visualized using UV irradiation ( $\lambda = 254$  nm). Flash column chromatography was performed with silica gel (particle size 0.100~0.200 mm) as the stationary phase. Preparative thin-layer chromatography was performed on 200 mm  $\times$  200 mm glass plates coated with 0.5 mm layer of silica gel 60. The nuclear magnetic resonance (NMR) spectra were recorded on Bruker 400 MHz NMR spectrometer. NMR spectra were processed using MestReNova v14.3.0. Chemical shifts ( $\delta$ ) were expressed in ppm referenced to the signals of residual of chloroform-*d* ( $^1\text{H}$ : 7.26 ppm,  $^{13}\text{C}$ : 77.16 ppm). Abbreviations: s = singlet, d = doublet, t = triplet, q = quartet, m = multiplet. Coupling constants ( $J$ ) were reported in Hertz. High-resolution mass spectra (HR MS) determinations were carried out on a Micromass GCT-TOF mass spectrometer with electron ionization (EI) source or a Xevo G2-XS-TOF mass spectrometer with atmospheric solids analysis probe (ASAP) source. Matrix-assisted laser desorption ionization-time of flight (MALDI-TOF) mass spectra (MS) were measured on a Bruker Autoflex MALDI-TOF/TOF instrument using trans-2-(3-(4-(*t*-butyl)phenyl)-2-methyl-2-propenylidene)malononi-trile (DCTB) in  $\text{CHCl}_3$  as supporting matrix.

**Optical Property Characterization.** UV-vis absorption spectra were recorded on a Perkin-Elmer Lambda 950 spectrometer using a 10 mm quartz cuvette at 298 K. Spectrofluorometer Fluorolog-3 (HORIBA Jobin Yvon) was used for the fluorescence measurement. The PLQY values were obtained directly using a Quantaaurus-QY Plus UV-NIR absolute PL quantum yield spectrometer (Hamamatsu Photonics C13534-11) equipped with an integrating sphere.

**Single-Crystal X-ray Diffraction Analysis.** X-ray single-crystal data was collected at low temperatures on Burker D8 venture diffractometer using a copper or molybdenum radiation source. Single crystals of **DBA-1** were grown by slow diffusion of anhydrous ethanol into its deuterated chloroform solution. Single crystals of **DBA-2** were grown by slow evaporation of its *n*-hexane solution. Single crystals of **DBA-3** and **DBA-4** were obtained by slow diffusion of anhydrous methanol into its solution in deuterated chloroform and ethyl acetate. All the crystals were obtained at room temperature.

**Theoretical Calculation.** Theoretical calculations were carried out using the Gaussian 09 (Revision D.01) suite of program.<sup>1</sup> All calculations were performed using the density functional theory (DFT) with Becke's three-parameter hybrid exchange functionals and the Lee-Yang-Parr correlation functional (B3LYP) employing the 6-31G(d,p) basis set for all atoms.<sup>2,3</sup> Time dependent DFT (TD-DFT) calculations were performed at the B3LYP/6-31G(d,p) level of theory using the polarizable continuum model (PCM) assuming chloroform as solvent. NICS values were calculated using the standard GIAO (GIAO=NMR) method<sup>4,5</sup> at the level of B3LYP/6-31G(d,p).

**Charge-Carrier Mobility Measurement.** The devices with a structure of glass/ITO/PEDOT:PSS/active layer/MoO<sub>3</sub>/Ag were fabricated to measure the hole mobility. The ITO-coated glass was pre-cleaned and modified by a thin layer of PEDOT:PSS which was spin-cast from a PEDOT:PSS aqueous solution (Baytron P VP AI4083 from H. C. Stark) at 5000 rpm for 40 s, and then dried at 150 °C for 15 min in air. The thickness of the PEDOT:PSS layer is about 30 nm. The active layer was spin-coated from chloroform solution (10 mg/mL) onto the PEDOT:PSS layer at the speed of 2000 rpm, giving the thickness of 100 nm approximately. After the deposition of the active layer, about 10 nm of MoO<sub>3</sub> layer was deposited at a pressure of  $2.0 \times 10^{-5}$  Pa onto the active layer. Tin foil was used as blocking layers to protect cells from light during measurement. The device characteristics were extracted by modeling the dark current under forward bias using the space-charge-limited current expression described by the original Mott-Gurney equation:

$$J = \frac{9}{8} \epsilon_r \epsilon_0 \mu \frac{V^2}{L^3}$$

where  $\epsilon_r \approx 3$  is the average dielectric constant of the polymer blend,  $\epsilon_0$  is the permittivity of the free space,  $\mu$  is the charge-carrier mobility,  $V$  is the applied voltage, and  $L$  is the thickness of the film.

**Thin Film XRD Characterization.** The X-ray diffraction pattern was measured by Bruker D8 Advance Instrument, with a voltage of 40 kV, a current of 200 mA, Cu Ka radiation, and the sample substrate was a silicon substrate. For the fabrication of active layer films: The DBAs were dissolved in chloroform at 50 °C for 6 hours, and then spin-coated onto the silicon substrates at the speed of 2000 rpm. The measurement angle range is 2 to 30 degrees.

**Thermal Properties Analysis.** Thermogravimetric analysis (TGA) was carried out by using METTLER TOLEDO TGA1 under nitrogen atmosphere at a heating rate of 10 °C/min. Differential scanning calorimetry (DSC) spectra were recorded on a METTLER TOLEDO DSC1 device at a heating/cooling rate of 10 °C/min under nitrogen atmosphere.

**Electrochemical Characterization.** Cyclic voltammetry was performed using a CHI750E analyzer with a scan rate of 100 mV/s at room temperature. The electrolytic cell was a conventional three-electrode cell with a glassy carbon working electrode, a platinum wire counter electrode, and a silver wire reference electrode. The measurement of oxidation potentials was performed in dry dichloromethane with 0.4 M of tetra-*n*-butylammonium hexafluorophosphate (*n*-Bu<sub>4</sub>N<sup>+</sup>PF<sub>6</sub><sup>-</sup>) as supporting electrolyte.

## Synthetic Procedures

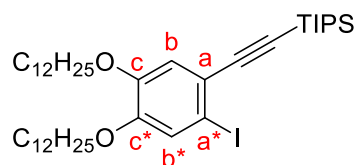
Compound **5**<sup>6</sup> and **6**<sup>7</sup> were synthesized following procedures reported in the literature.

**1,2-Bis(*n*-dodecyloxy)-4-iodo-5-(triisopropylsilyl)ethynylbenzene (1) and 1,2-Bis(dodecyloxy)-4,5-bis[(triisopropylsilyl)ethynyl]benzene (2)**

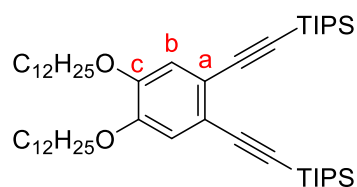
1,2-Bis(*n*-dodecyloxy)-4,5-diiodobenzene **5** (417mg, 0.597 mmol), Pd(PPh<sub>3</sub>)<sub>2</sub>Cl<sub>2</sub>

(28.0 mg, 39.9  $\mu\text{mol}$ ), CuI (13.1 mg, 68.8  $\mu\text{mol}$ ) and  $\text{NEt}_3$  (10 mL) were placed respectively in a two-necked round-bottom flask under argon atmosphere. A solution of (triisopropylsilyl)acetylene (120 mg, 0.657 mmol) in  $\text{NEt}_3$  (2 mL) was added slowly via a syringe over 5 h while keeping the reaction temperature at 40  $^\circ\text{C}$ . After stirring the mixture for another 14 h, the cooled mixture was concentrated in vacuo, then suspended in  $\text{CH}_2\text{Cl}_2/n\text{-hexane}$  (2 mL/5 mL) and filtered through a short bed of silica gel. Upon evaporation of the filtrate, the crude was purified by silica gel column chromatography (eluent: *n*-hexane) to furnish compound **1** (144 mg, 35%) and **2** (174 mg, 65%) both as pale-yellow oil.

**1**:  $^1\text{H}$  NMR (400 MHz,  $\text{CDCl}_3$ , 298 K)  $\delta$  7.20 (s, 1H,  $\text{H}^{b^*}$ ), 6.95 (s, 1H,  $\text{H}^b$ ), 3.99 – 3.91 (m, 4H,  $\text{H}^{\text{dodec-}}$ ), 1.85 – 1.74 (m, 4H,  $\text{H}^{\text{dodec-}}$ ), 1.50 – 1.39 (m, 4H,  $\text{H}^{\text{dodec-}}$ ), 1.39 – 1.21 (m, 32H,  $\text{H}^{\text{dodec-}}$ ), 1.16 (s, 21H,  $\text{H}^{\text{TIPS-}}$ ), 0.88 (t,  $J = 6.8$  Hz, 6H,  $\text{H}^{\text{dodec-}}$ );  $^{13}\text{C}$  NMR (101 MHz,  $\text{CDCl}_3$ , 298 K)  $\delta$  150.1, 148.9, 122.9, 122.3, 117.6, 108.4, 92.9, 90.4, 69.5, 32.1, 29.8, 29.8, 29.8, 29.7, 29.5, 29.5, 29.2, 29.2, 26.1, 26.1, 22.8, 18.9, 14.3, 11.5; HR MS (ASAP): calcd for  $\text{C}_{41}\text{H}_{74}\text{IO}_2\text{Si}$ ,  $m/z = 753.4503$ ; found 753.4510  $[\text{M} + \text{H}]^+$ .

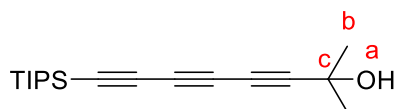


**2**:  $^1\text{H}$  NMR (400 MHz,  $\text{CDCl}_3$ , 298 K)  $\delta$  6.88 (s, 2H,  $\text{H}^b$ ), 3.97 (t,  $J = 6.6$  Hz, 4H,  $\text{H}^{\text{dodec-}}$ ), 1.86 – 1.74 (m, 4H,  $\text{H}^{\text{dodec-}}$ ), 1.51 – 1.39 (m, 4H,  $\text{H}^{\text{dodec-}}$ ), 1.39 – 1.22 (m, 32H,  $\text{H}^{\text{dodec-}}$ ), 1.12 (s, 42H,  $\text{H}^{\text{TIPS-}}$ ), 0.92 – 0.84 (m, 6H,  $\text{H}^{\text{dodec-}}$ );  $^{13}\text{C}$  NMR (101 MHz,  $\text{CDCl}_3$ , 298 K)  $\delta$  149.2, 118.7, 117.7, 105.8, 92.9, 69.4, 32.1, 29.8, 29.8, 29.8, 29.5, 29.5, 29.2, 26.1, 22.9, 18.9, 14.3, 11.5; HR MS (ASAP): calcd for  $\text{C}_{52}\text{H}_{95}\text{IO}_2\text{Si}_2$ ,  $m/z = 806.6871$ ; found 806.6871  $[\text{M} + \text{H}]^+$ .



## 2-Methyl-8-(triisopropylsilyl)octa-3,5,7-triyn-2-ol (**7**)

To a solution of compound **6** (2.10 g, 7.94 mmol) dissolved in anhydrous THF (10 mL) was added dropwise TBAF (1.58 mL, 1 M in THF) at 0  $^\circ\text{C}$ . After stirring the solution for 1 h at 0  $^\circ\text{C}$ , the reaction was quenched with  $\text{NH}_4\text{Cl}$  aq., followed by extracting with ether. The extract was separated, washed with brine and dried over anhydrous  $\text{MgSO}_4$ . The filtrate was evaporated, suspended in ethyl acetate/*n*-hexane (1/10, *v/v*) and filtered through a short bed of silica gel to furnish a brown oil of desilylated intermediate.

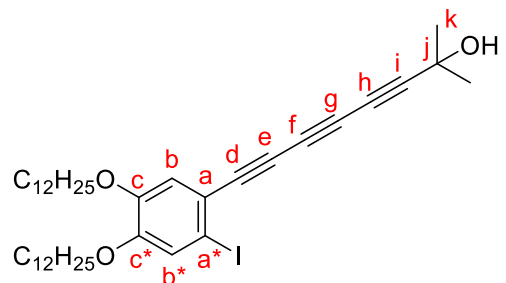


To a solution of the above desilylated intermediate dissolved in  $\text{MeOH}/\text{H}_2\text{O}$  ( $v/v = 2/1$ , 36 mL), *n*-butylamine (925 mg, 12.6 mmol), copper chloride (12.0 mg, 0.121 mmol) and hydroxylamine hydrochloride (88.0 mg, 1.20 mmol) were introduced respectively. The solution of (bromoethynyl)triisopropylsilane (1.10 g, 4.21 mmol) in methanol (8 mL) was added dropwise, followed by stirring for 14 h. The mixture was diluted with water, extracted with ether. The separated organics was washed with brine, dried over  $\text{MgSO}_4$  and concentrated. The residue was purified by flash column chromatography on silica gel (ethyl acetate/*n*-hexane = 1/10, *v/v*) to give the title compound (1.07 g, 88%) as a light rufous solid.  $^1\text{H}$  NMR (400 MHz,  $\text{CDCl}_3$ , 298 K)  $\delta$

1.92 (s, 1H, H<sup>a</sup>), 1.54 (s, 6H, H<sup>b</sup>), 1.08 (s, 21H, H<sup>TIPS-</sup>); <sup>13</sup>C NMR (101 MHz, CDCl<sub>3</sub>, 298 K) δ 89.6, 85.5, 82.1, 77.5, 77.4, 77.2, 76.8, 67.6, 65.8, 64.6, 60.1, 31.1, 18.6, 11.4; HR MS (EI): calcd for C<sub>18</sub>H<sub>28</sub>OSi, *m/z* = 289.1988; found, 289.1988 [M]<sup>+</sup>.

### 1,2-Bis(dodecyloxy)-4-iodo-5-[(1-methyl-1-hydroxyethyl)octyltriy-nyl]benzene (3)

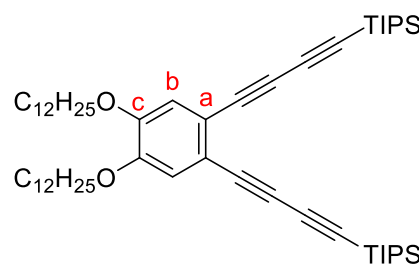
A two-necked round-bottom flask was charged with a solution of 1,2-bis(*n*-dodecyloxy)-4,5-diiodobenzene **7** (4.36 g, 6.24 mmol) in THF (15 mL), Pd(PPh<sub>3</sub>)<sub>4</sub> (120 mg, 0.104 mol) and CuI (119 mg, 0.625 mol) and TBAF (2.08 mL, 1.0 M in THF). The solution of hexatriyne **7** (598 mg, 2.07 mmol) in *i*-Pr<sub>2</sub>NH (50 mL) was added



dropwise through a pressure-equalizing dropping funnel over 5 h at room temperature. The reaction was monitored by TLC (eluent: *n*-hexane/dichloromethane = 1/1, *v/v*) until completion. After concentrating the mixture under reduced pressure, the residue was purified by column chromatography (eluent: *n*-hexane/dichloromethane = 1/1, *v/v*) to give compound **3** (555 mg, 38%) as reddish-brown solid. <sup>1</sup>H NMR (400 MHz, CDCl<sub>3</sub>, 298 K) δ 7.17 (s, 1H, H<sup>b\*</sup>), 6.96 (s, 1H, H<sup>b</sup>), 4.00 – 3.88 (m, 4H, H<sup>dodec-</sup>), 2.02 (s, 1H, H<sup>l</sup>), 1.86 – 1.73 (m, 4H, H<sup>dodec-</sup>), 1.56 (s, 6H, H<sup>k</sup>), 1.48 – 1.39 (m, 4H, H<sup>dodec-</sup>), 1.36 – 1.17 (m, 32H, H<sup>dodec-</sup>), 0.88 (t, *J* = 6.7 Hz, 6H, H<sup>dodec-</sup>); <sup>13</sup>C NMR (101 MHz, CDCl<sub>3</sub>, 298 K) δ 151.3, 148.9, 122.7, 119.4, 118.2, 91.1, 84.5, 79.1, 76.0, 69.4, 69.4, 67.8, 67.0, 65.9, 63.9, 32.1, 31.1, 29.8, 29.8, 29.7, 29.7, 29.5, 29.5, 29.5, 29.1, 29.1, 26.0, 26.0, 22.8, 14.3; HR MS (ASAP): calcd for C<sub>39</sub>H<sub>60</sub>IO<sub>3</sub>, *m/z* = 703.3587; found 703.3584 [M + H]<sup>+</sup>.

### 1,2-Bis(dodecyloxy)-4,5-bis[(triisopropylsilyl)butadiynyl]benzene (4)

To a Schlenk tube charged with compound **5** (700 mg, 1.00 mmol), butadiyne **9** (689 mg, 2.61 mmol), Pd(PPh<sub>3</sub>)<sub>4</sub> (58.0 mg, 50.2 μmol), CuI (57.0 mg, 299 μmol) and benzyltriethylammonium chloride (TEBAC) (68.0 mg, 299 μmol) was added toluene (10 mL) and aqueous solution of KOH (2.6 mL, 5.0 M). The reaction was stirred at 80 °C and

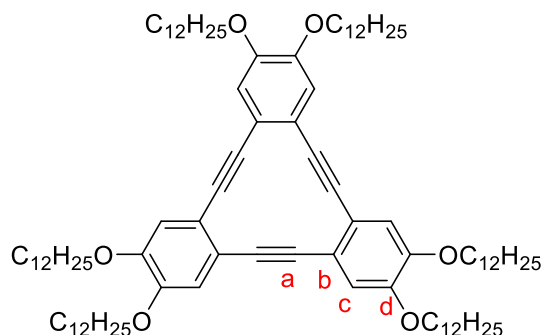


monitored by TLC (eluent: dichloromethane/*n*-hexane = 1/30, *v/v*). After completion of the reaction, 1 M HCl aq. was poured into the cooled mixture, followed by extraction with ether. The organic phase was separated, combined and washed with water, brine, dried over MgSO<sub>4</sub> and evaporated in vacuo. The residue was purified by column chromatography over silica gel (eluent: dichloromethane/*n*-hexane = 1/30, *v/v*) to obtain compound **4** (394 mg, 46%) as brown oil. <sup>1</sup>H NMR (400 MHz, CDCl<sub>3</sub>, 298 K) δ 6.92 (s, 2H, H<sup>b</sup>), 3.95 (t, *J* = 6.6 Hz, 4H, H<sup>dodec-</sup>), 1.85 - 1.74 (m, 4H, H<sup>dodec-</sup>), 1.47 - 1.39 (m, 4H, H<sup>dodec-</sup>), 1.38 - 1.19 (m, 32H, H<sup>dodec-</sup>), 1.11 (s, 42H, H<sup>TIPS-</sup>), 0.88 (t, *J* = 6.6 Hz, 6H, H<sup>dodec-</sup>); <sup>13</sup>C NMR (101 MHz, CDCl<sub>3</sub>, 298 K) δ 149.9, 118.4, 116.8, 89.8, 89.0, 74.0, 69.3, 32.1, 29.8, 29.8, 29.7, 29.7, 29.5, 29.5, 29.1, 26.1, 22.8, 18.7, 14.3, 11.5; HR

MS (ASAP): calcd for C<sub>56</sub>H<sub>95</sub>O<sub>2</sub>Si<sub>2</sub>,  $m/z$  = 855.6871; found 855.6873 [M + H]<sup>+</sup>.

### DBA-1

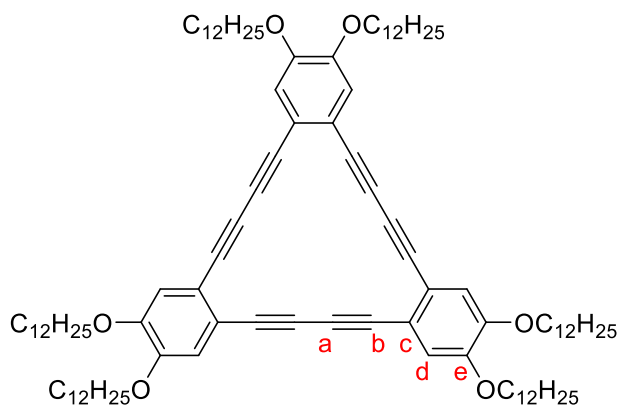
To a solution of compound **1** (354 mg, 0.470 mmol) dissolved in THF (5 mL) was added TBAF (0.94 mL, 1 M in THF) dropwise using a syringe. After stirring at room temperature for 1 h, the mixture was diluted with water and extracted with ether. The separated organic phase was washed with water for four times and dried over anhydrous MgSO<sub>4</sub>. The filtrate was concentrated under vacuo, suspended in *n*-hexane, and then filtered over a short cake of silica gel. The collected *n*-hexane solution was evaporated to afford deprotected intermediate as gray powder.



A suspension of CuI (84.0 mg, 0.441 mmol) and K<sub>2</sub>CO<sub>3</sub> (36.0 mg, 0.261 mmol) in DMF (5 mL) was stirred at room temperature for 1 h, before slowly adding DMF (3.5 mL) solution of the deprotected intermediate prepared above. After stirring at room temperature for 4 h, the reaction was heated to 140 °C and monitored by TLC. Upon completion of the reaction, the mixture was cooled and concentrated in vacuum. The residue was suspended in dichloromethane, passed through a short silica gel column (eluent: dichloromethane), and the solvent was evaporated under reduced pressure. The crude product was purified by flash column chromatography over silica gel (eluent: dichloromethane/*n*-hexane = 3:7, *v/v*), followed by preparative thin layer chromatography (silica gel, eluent: dichloromethane/*n*-hexane = 1:8, *v/v*) to obtain **DBA-1** (65.0 mg, 29%) as yellow solid. <sup>1</sup>H NMR (400 MHz, CDCl<sub>3</sub>, 298 K) δ 6.72 (s, 6H, H<sup>c</sup>), 3.95 (t, *J* = 6.6 Hz, 12H, H<sup>dodec-</sup>), 1.85 – 1.76 (m, 12H, H<sup>dodec-</sup>), 1.49 – 1.41 (m, 12H, H<sup>dodec-</sup>), 1.34 – 1.20 (m, 96H, H<sup>dodec-</sup>), 0.88 (t, *J* = 6.6 Hz, 18H, H<sup>dodec-</sup>); <sup>13</sup>C NMR (101MHz, CDCl<sub>3</sub>, 298 K) δ 149.2, 119.8, 115.8, 92.0, 69.2, 32.1, 29.9, 29.8, 29.8, 29.5, 29.5, 29.3, 26.1, 22.8, 14.3; MALDI-TOF MS: calcd for C<sub>96</sub>H<sub>156</sub>O<sub>6</sub>,  $m/z$  = 1405.190; found 1405.366 [M]<sup>+</sup>. The spectroscopic data agree with that reported in the literature.<sup>6</sup>

### DBA-2

To a solution of compound **2** (646 mg, 0.800 mmol) in THF (7 mL), TBAF (3.2 mL, 1.0 M in THF) was added dropwise at 0 °C. After stirring for 1 h, water was added to dilute the reaction mixture. Subsequently, the mixture was extracted with ethyl ether. The organic phase was washed with water, dried over MgSO<sub>4</sub>, and evaporated under reduced pressure. The residue was suspended in petroleum ether,

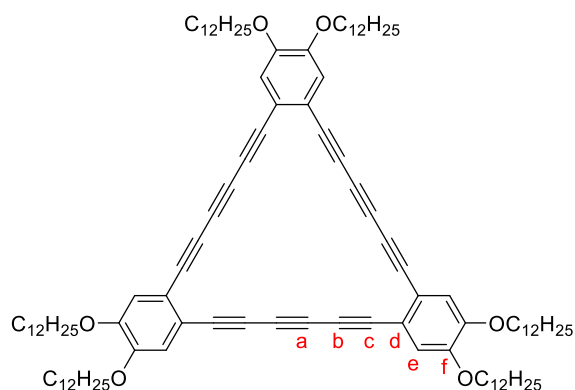


filtered through a short bed of silica gel, and then the organic solvent was evaporated to afford the desilylated product as gray powder.

To a mixture of desilylated product, Pd (PPh<sub>3</sub>)<sub>2</sub>Cl<sub>2</sub> (47.0 mg, 66.7 μmol), CuI (33.0 mg, 0.173 mmol) and I<sub>2</sub> (170 mg, 667 μmol) was added a mixed solvent of THF/*i*-Pr<sub>2</sub>NH (*v/v* = 1/1, 250 mL). The reaction solution was stirred at room temperature for 13 h and monitored by TLC. Upon completion of the reaction, the mixture was concentrated in vacuum, and the residue was redissolved in diethyl ether. The organic phase was washed with Na<sub>2</sub>SO<sub>3</sub> aq., water and brine. The solution was dried over MgSO<sub>4</sub> and evaporated under reduced pressure. The residue was purified by flash column chromatography over silica gel (dichloromethane/*n*-hexane = 1/4 – 3/7, *v/v*) and preparative thin layer chromatography on SiO<sub>2</sub> (dichloromethane/*n*-hexane = 1/4 – 3/7, *v/v*), followed by reprecipitation from chloroform/methanol (*v/v*, 1/8) to give **DBA-2** (62.0 mg, 16%) as gray powder. <sup>1</sup>H NMR (400 MHz, CDCl<sub>3</sub>, 298 K) δ 7.10 (s, 6H, H<sup>d</sup>), 4.03 (t, *J* = 6.6 Hz, 12H, H<sup>dodec-</sup>), 1.90 – 1.78 (m, 12H, H<sup>dodec-</sup>), 1.51 – 1.43 (m, 12H, H<sup>dodec-</sup>), 1.39 – 1.23 (m, 96H, H<sup>dodec-</sup>), 0.88 (t, *J* = 6.7 Hz, 18H, H<sup>dodec-</sup>); <sup>13</sup>C NMR (101 MHz, CDCl<sub>3</sub>, 298 K) δ 149.9, 118.5, 116.1, 81.1, 77.1, 69.4, 32.1, 29.8, 29.8, 29.8, 29.5, 29.1, 26.1, 22.8, 14.3; MALDI-TOF MS: calcd for C<sub>102</sub>H<sub>156</sub>O<sub>6</sub>, *m/z* = 1477.190; found 1477.189 [M]<sup>+</sup>. The spectroscopic data agree with that reported in the literature.<sup>8</sup>

### DBA-3

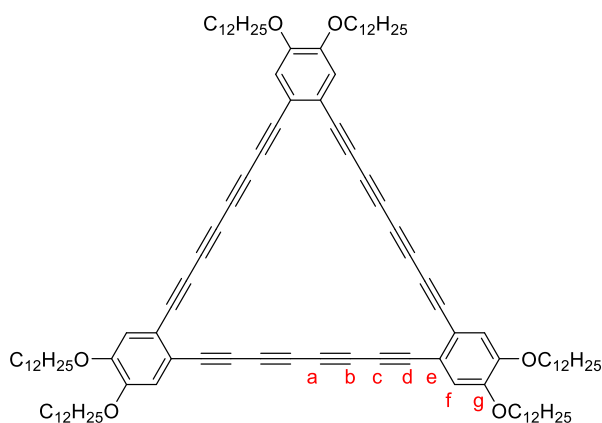
To a stirred solution of triyne precursor **3** (555 mg, 0.790 mmol) dissolved in toluene (10 mL) was added Pd(PPh<sub>3</sub>)<sub>4</sub> (46.0 mg, 39.8 μmol), CuI (46.0 mg, 0.242 mmol), TEBAC (55.0 mg, 0.241 mmol) and KOH aq. (0.8 mL, 5.0 M). The reaction mixture was heated at 65 °C for 14 h and monitored by TLC. Upon completion of the reaction, the mixture was cooled, poured into 1 M



HCl aq., and extracted with ether. The separated organic phase was washed with water, brine and dried over MgSO<sub>4</sub>. After evaporation of the solvent in vacuo, the crude product was purified by silica gel column chromatography (dichloromethane/*n*-hexane = 1/4, *v/v*), followed by reprecipitation from dichloromethane/methanol (1/8, *v/v*) to give **DBA-3** (24.0 mg, 6%) as claybank powder. <sup>1</sup>H NMR (400 MHz, CDCl<sub>3</sub>, 298 K) δ 6.83 (s, 6H, H<sup>e</sup>), 3.96 (t, *J* = 6.6 Hz, 12H, H<sup>dodec-</sup>), 1.86 – 1.75 (m, 12H, H<sup>dodec-</sup>), 1.48 – 1.39 (m, 12H, H<sup>dodec-</sup>), 1.27 (d, *J* = 8.4 Hz, 96H, H<sup>dodec-</sup>), 0.88 (t, *J* = 6.7 Hz, 18H, H<sup>dodec-</sup>); <sup>13</sup>C NMR (101 MHz, CDCl<sub>3</sub>, 298 K) δ 150.3, 118.8, 116.6, 77.8, 69.3, 68.1, 32.1, 29.8, 29.8, 29.7, 29.7, 29.5, 29.5, 29.0, 26.0, 22.8, 14.3; MALDI-TOF MS: calcd for C<sub>108</sub>H<sub>156</sub>O<sub>6</sub>, *m/z* = 1549.190; found 1549.205 [M]<sup>+</sup>.

#### DBA-4

To a solution of compound **4** (467 mg, 0.546 mmol) in THF (5 mL) was added slowly TBAF (1.7 mL, 1.0 M in THF) at 0 °C, followed by stirring for 1 h. Upon completion of the deprotection, the mixture was diluted with water, extracted with diethyl ether, dried over MgSO<sub>4</sub> and the filtrate was evaporated. The residue was redissolved in *n*-hexane, passed through a short silica gel column (eluent: dichloromethane/*n*-hexane = 1/20, *v/v*). After evaporation, the desilylated product was obtained as claybank powder.



To a mixture of the above powder, Pd (PPh<sub>3</sub>)<sub>2</sub>Cl<sub>2</sub> (32.0 mg, 45.6 μmol), CuI (18.0 mg, 94.5 μmol) and I<sub>2</sub> (124 mg, 0.489 mmol) was added a mixture solvent of THF/*i*-Pr<sub>2</sub>NH (*v/v* = 1/1, 172 mL). The solution was stirred at room temperature for 16 h and the reaction was monitored by TLC. Upon completion of the reaction, the mixture was concentrated in vacuum and the residue was redissolved in diethyl ether. After washing with Na<sub>2</sub>SO<sub>3</sub> aq., water and brine respectively, the organic phase was dried over MgSO<sub>4</sub> and evaporated under reduced pressure. The residue was purified by silica gel column chromatography (eluent: dichloromethane/*n*-hexane = 1/4, *v/v*) and preparative thin layer chromatography (silica gel, eluent: dichloromethane/*n*-hexane = 3/7, *v/v*), followed by reprecipitation from chloroform/methanol (*v/v*, 1/8) to give **DBA-4** (17.0 mg, 6%) as gray powder. <sup>1</sup>H NMR (400 MHz, CDCl<sub>3</sub>, 298 K) δ 6.93 (s, 6H, H<sup>f</sup>), 3.98 (t, *J* = 6.6 Hz, 12H, H<sup>dodec-</sup>), 1.87 – 1.76 (m, 12H, H<sup>dodec-</sup>), 1.49 – 1.41 (m, 12H, H<sup>dodec-</sup>), 1.36 – 1.17 (m, 96H, H<sup>dodec-</sup>), 0.88 (t, *J* = 6.7 Hz, 18H, H<sup>dodec-</sup>); <sup>13</sup>C NMR (101 MHz, CDCl<sub>3</sub>, 298 K) δ 149.9, 118.4, 116.8, 89.8, 89.0, 74.0, 69.3, 32.1, 29.8, 29.8, 29.7, 29.7, 29.5, 29.5, 29.1, 26.1, 22.8, 18.7, 14.3; MALDI-TOF MS: calcd for C<sub>114</sub>H<sub>156</sub>O<sub>6</sub>, 1621.190; found 1621.302 [M]<sup>+</sup>.

## X-ray Single Crystal Structures

X-ray crystallographic analysis revealed residual electron density and elevated R-factors (see detail crystallographic data in **Figure S3-S7, Table S1-S4**), primarily attributed to dynamic disorder in some of the flexible *n*-dodecyl chains and inherent low crystal quality. Despite iterative optimization of crystallization conditions (e.g., solvent ratios, temperature gradients), crystals of higher quality still could not be obtained. Crucially, however, the core frameworks (DBA) exhibited well-resolved structural features, enabling robust analysis of their geometric and electronic characteristics in this study.

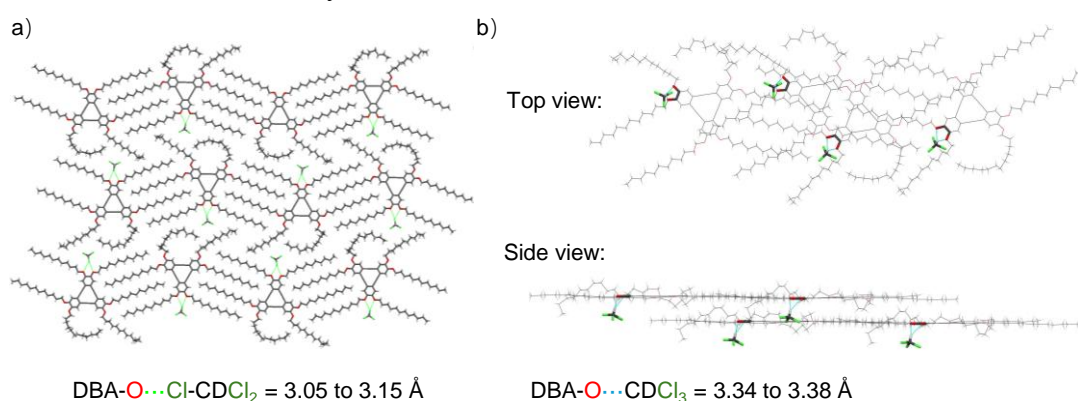


**Figure S1.** Packing structure of **DBA-1** in the crystal: a) 2D sheet-like packing structure with DBA-O...Cl-CDCl<sub>2</sub> interaction (green lines); b) top and side view of DBA-O...D-CCl<sub>3</sub> interaction (blue lines) between two neighboring layers. C: black; Cl: green; O: red.

### Crystallographic Data of **DBA-1** (CCDC: 2441877)

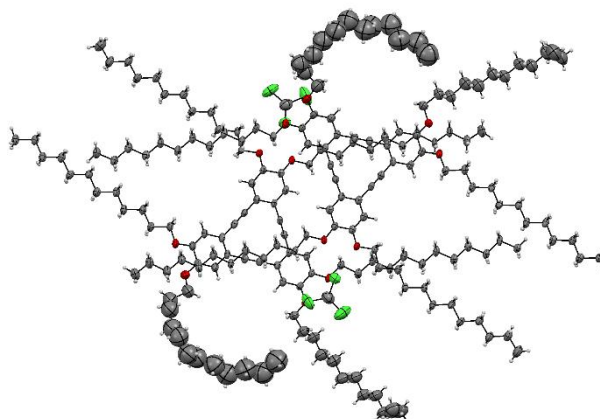


**Figure S2.** Crystal structure of **DBA-1** with thermal ellipsoids shown at 50% probability. Atom colors: H, white; C, black; O, red; Cl, green.

**Table S1.** Crystal data and structure refinement for **DBA-1**

Empirical formula	4(CDCl <sub>3</sub> ), 2(C <sub>96</sub> H <sub>155</sub> O <sub>6</sub> )
Formula weight	6128.30
Temperature/K	150
Crystal system	triclinic

Space group	P-1
a/Å	12.4280(11)
b/Å	49.394(5)
c/Å	15.1665(12)
$\alpha/^\circ$	90
$\beta/^\circ$	93.045(7)
$\gamma/^\circ$	90
Volume/Å <sup>3</sup>	9297.1(15)
Z	1
$\rho_{\text{calc}}$ (g/cm <sup>3</sup> )	1.095
$\mu/\text{mm}^{-1}$	1.265
F(000)	3366
Crystal size/mm <sup>3</sup>	0.2 × 0.2 × 0.2
Crystal shape	plate
Crystal color	pale green
Radiation	Cu K $\alpha$ ( $\lambda$ = 1.54184)
2 $\Theta$ range for data collection/ $^\circ$	2.684 to 74.590
Index ranges	-12 ≤ h ≤ 14, -60 ≤ k ≤ 53, -18 ≤ l ≤ 18
Reflections collected	54631
Independent reflections	29356[R <sub>int</sub> = 0.2276]
Data/restraints/parameters	29356/ 1496/ 1927
Goodness-of-fit on F <sup>2</sup>	1.039
Final R indexes [I ≥ 2 $\sigma$ (I)]	R <sub>1</sub> = 0.1525, wR <sub>2</sub> = 0.3622
Final R indexes [all data]	R <sub>1</sub> = 0.3639, wR <sub>2</sub> = 0.5023
Largest diff. peak/hole / e Å <sup>-3</sup>	0.778/ -0.460

### Crystallographic Data of DBA-2 (CCDC: 2441874).

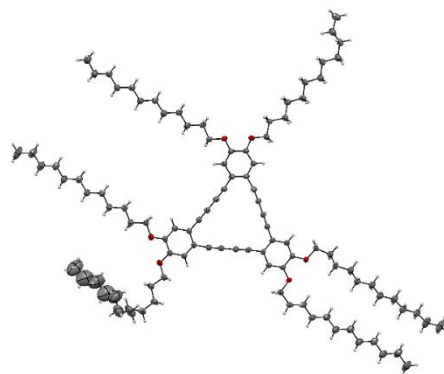


**Figure S3.** Crystal structure of **DBA-2** with thermal ellipsoids shown at 50% probability. Atom colors: H, white; C, black; O, red.

**Table S2.** Crystal data and structure refinement for **DBA-2**

Empirical formula	C <sub>102</sub> H <sub>156</sub> O <sub>6</sub>
Formula weight	1478.26
Temperature/K	193
Crystal system	triclinic
Space group	P-1
a/Å	12.9702(8)

b/Å	15.4584(11)
c/Å	24.0812(15)
$\alpha$ /°	82.398(3)
$\beta$ /°	83.216(2)
$\gamma$ /°	78.517(2)
Volume/Å <sup>3</sup>	4669.0(5)
Z	1
$\rho_{\text{calc}}$ (g/cm <sup>3</sup> )	1.051
$\mu$ /mm <sup>-1</sup>	1.265
F(000)	1632
Crystal size/mm <sup>3</sup>	0.1 × 0.2 × 0.3
Crystal shape	plate
Crystal color	colorless
Radiation	Mo K $\alpha$ ( $\lambda$ = 0.71073)
2 $\Theta$ range for data collection/°	1.714 to 27.560
Index ranges	-16 ≤ h ≤ 16, -20 ≤ k ≤ 20, -28 ≤ l ≤ 31
Reflections collected	44213
Independent reflections	21355 [R <sub>int</sub> = 0.0776, R <sub>sigma</sub> = 0.0826]
Data/restraints/parameters	21355/673/979
Goodness-of-fit on F <sup>2</sup>	1.015
Final R indexes [I ≥ 2 $\sigma$ (I)]	R <sub>1</sub> = 0.0900 wR <sub>2</sub> = 0.1868
Final R indexes [all data]	R <sub>1</sub> = 0.2134, wR <sub>2</sub> = 0.2499
Largest diff. peak/hole / e Å <sup>-3</sup>	0.716/-0.474

### Crystallographic Data of DBA-3 (CCDC: 2441875).

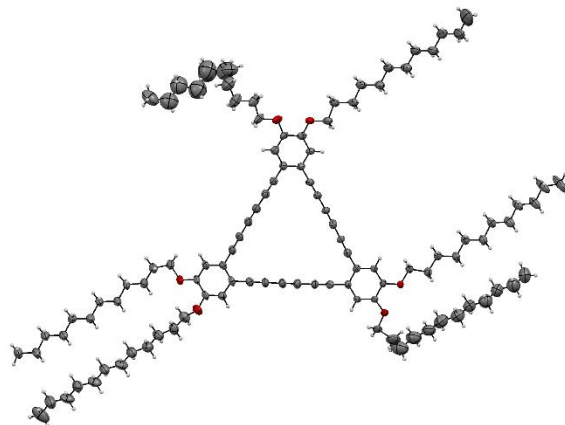


**Figure S4.** Crystal structure of **DBA-3** with thermal ellipsoids shown at 50% probability. Atom colors: H, white; C, black; O, red.

**Table S3.** Crystal data and structure refinement for **DBA-3**

Empirical formula	C108 H156 O6
Formula weight	1550.32
Temperature/K	193
Crystal system	triclinic
Space group	P-1
a/Å	13.1696(9)
b/Å	16.0193(11)

c/Å	24.6277(16)
$\alpha$ /°	99.486(2)
$\beta$ /°	99.832(2)
$\gamma$ /°	94.142(2)
Volume/Å <sup>3</sup>	5022.3(6)
Z	2
$\rho_{\text{calc}}$ (g/cm <sup>3</sup> )	1.025
$\mu$ /mm <sup>-1</sup>	0.061
F(000)	1704
Crystal size/mm <sup>3</sup>	0.1 × 0.2 × 0.2
Crystal shape	plate
Crystal color	light yellow
Radiation	Mo K $\alpha$ ( $\lambda$ = 0.71073)
2 $\Theta$ range for data collection/°	1.963 to 24.712
Index ranges	-15 ≤ h ≤ 15, -18 ≤ k ≤ 18, -24 ≤ l ≤ 28
Reflections collected	33160
Independent reflections	16666 [R <sub>int</sub> = 0.1272]
Data/restraints/parameters	16666/241/1033
Goodness-of-fit on F <sup>2</sup>	1.220
Final R indexes [I ≥ 2 $\sigma$ (I)]	R <sub>1</sub> = 0.1417, wR <sub>2</sub> = 0.3572
Final R indexes [all data]	R <sub>1</sub> = 0.2224, wR <sub>2</sub> = 0.4261
Largest diff. peak/hole / e Å <sup>-3</sup>	1.007/-0.542

### Crystallographic Data of DBA-4 (CCDC: 2441876).

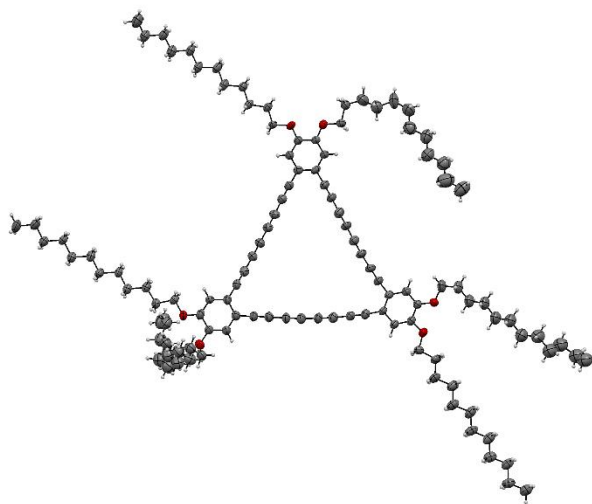


**Figure S5.** Crystal structure of **DBA-4** with thermal ellipsoids shown at 50% probability. Atom colors: H, white; C, black; O, red.

**Table S4.** Crystal data and structure refinement for **DBA-4**

Empirical formula	C <sub>114</sub> H <sub>156</sub> O <sub>6</sub>
Formula weight	1622.38
Temperature/K	223
Crystal system	triclinic
Space group	P-1
a/Å	14.182(4)

b/Å	17.405(6)
c/Å	22.946(9)
$\alpha$ /°	76.09(3)
$\beta$ /°	72.19(3)
$\gamma$ /°	76.66(3)
Volume/Å <sup>3</sup>	5158(3)
Z	2
$\rho_{\text{calc}}$ (g/cm <sup>3</sup> )	1.045
$\mu$ /mm <sup>-1</sup>	0.472
F(000)	1776
Crystal size/mm <sup>3</sup>	0.2 × 0.1 × 0.2
Crystal shape	plate
Crystal color	light yellow
Radiation	Cu K $\alpha$ ( $\lambda$ = 1.54178)
2 $\Theta$ range for data collection/°	2.057 to 68.667
Index ranges	-14 ≤ h ≤ 17, -20 ≤ k ≤ 21, -26 ≤ l ≤ 27
Reflections collected	41901
Independent reflections	16958[R <sub>int</sub> = 0.1410]
Data/restraints/parameters	16958/741087
Goodness-of-fit on F <sup>2</sup>	1.061
Final R indexes [I >= 2 $\sigma$ (I)]	R <sub>1</sub> = 0.1176, wR <sub>2</sub> = 0.3201
Final R indexes [all data]	R <sub>1</sub> = 0.2352, wR <sub>2</sub> = 0.4227
Largest diff. peak/hole / e Å <sup>-3</sup>	0.631/-0.804

## DFT Calculations

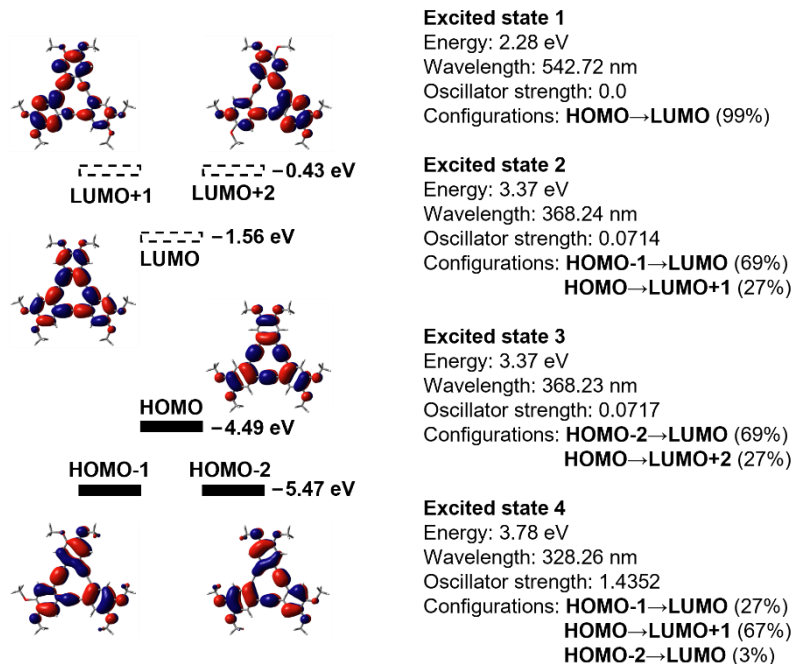


**Figure S6.** The molecular orbitals (isovalue = 0.02), energy levels, excitation energies and oscillator strengths of **DBA-1'**, calculated at the TD-DFT (B3LYP/6-31G(d,p)) level of theory.

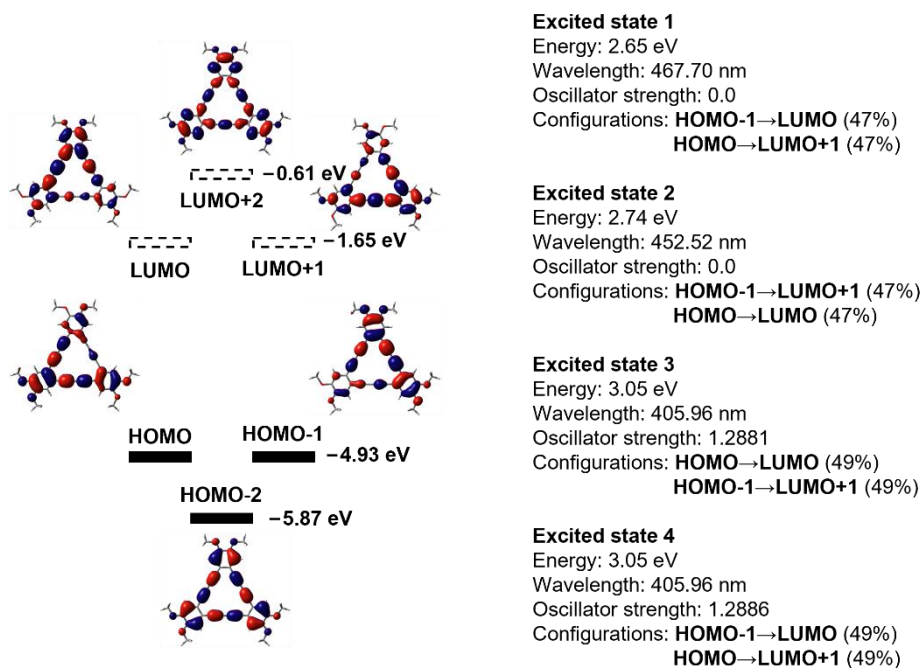


**Figure S7.** The molecular orbitals (isovalue = 0.02), energy levels, excitation energies and oscillator strengths of **DBA-2'**, calculated at the TD-DFT (B3LYP/6-31G(d,p)) level of theory.

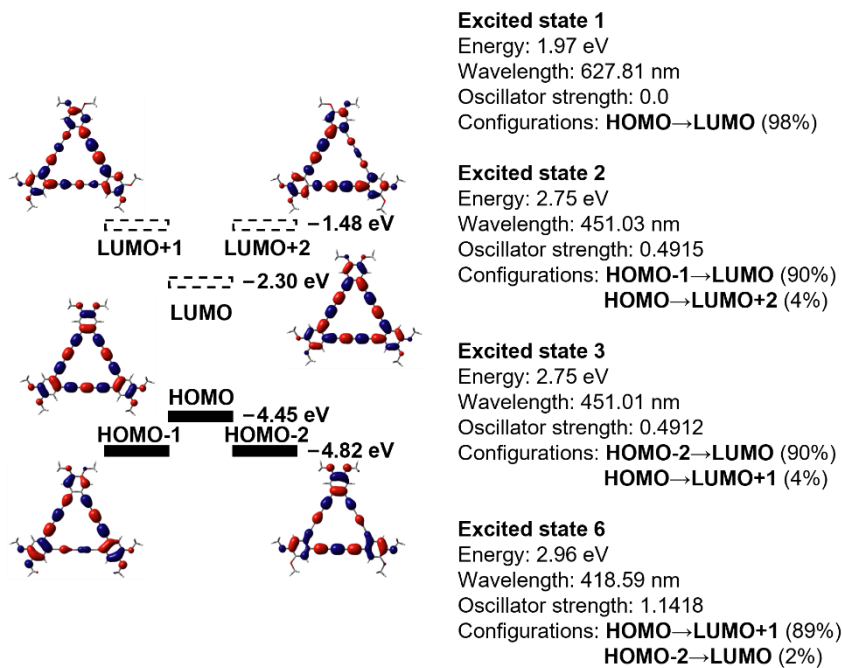


**Figure S8.** The molecular orbitals (isovalue = 0.02), energy levels, excitation energies and oscillator strengths of DBA-3', calculated at the TD-DFT (B3LYP/6-31G(d,p)) level of theory.

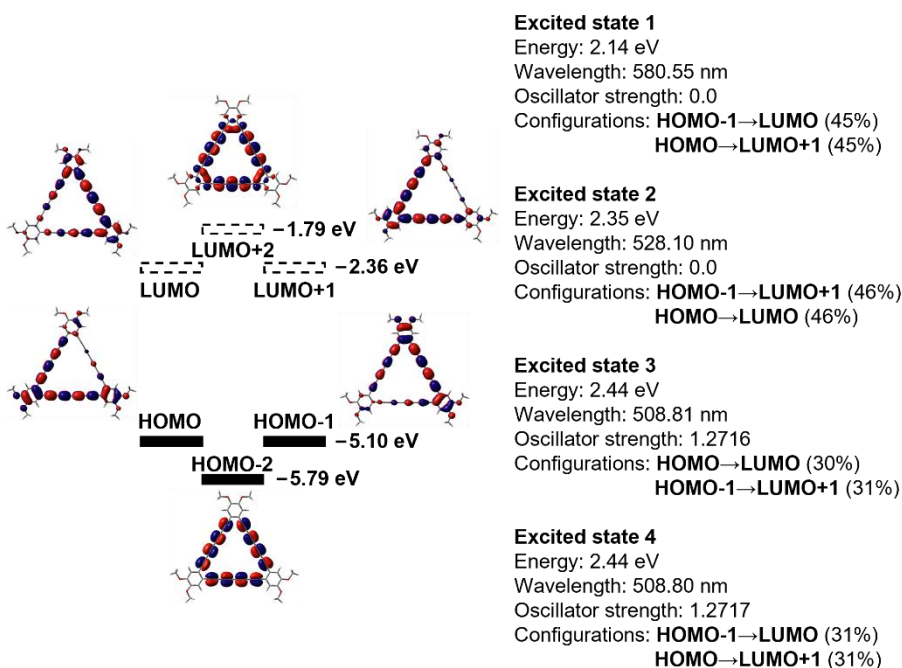


**Figure S9.** The molecular orbitals (isovalue = 0.02), energy levels, excitation energies and oscillator strengths of DBA-4', calculated at the TD-DFT (B3LYP/6-31G(d,p)) level of theory.

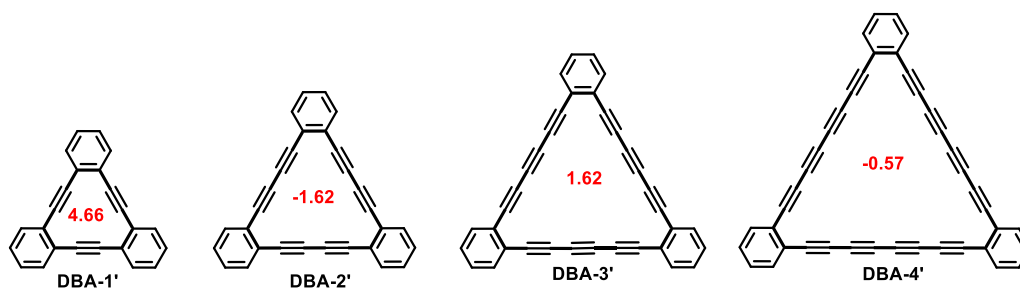


**Figure S10.** DFT calculated NICS(1) values of DBA-n' (n = 1~4) at the B3LYP/6-31G(d,p) level of theory. The methoxy groups were omitted for clarity.

## UV-vis Absorption Spectra

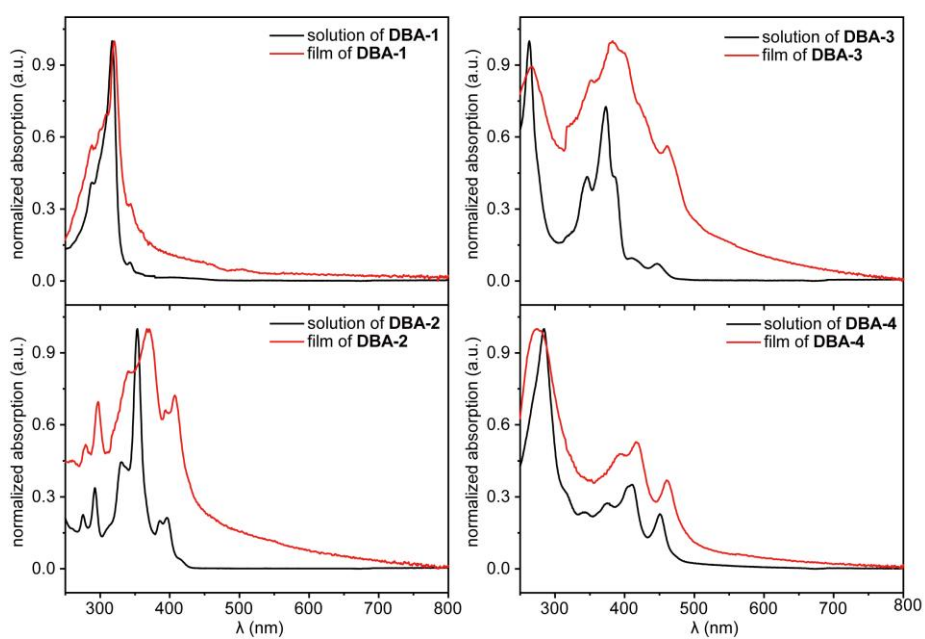


**Figure S11.** Comparison of UV-vis absorption spectra of DBA-n (n = 1~4) in solution ( $10^{-6}$  mol/L in  $\text{CHCl}_3$ , 298 K) and neat films.

## Hole Mobility Measurements

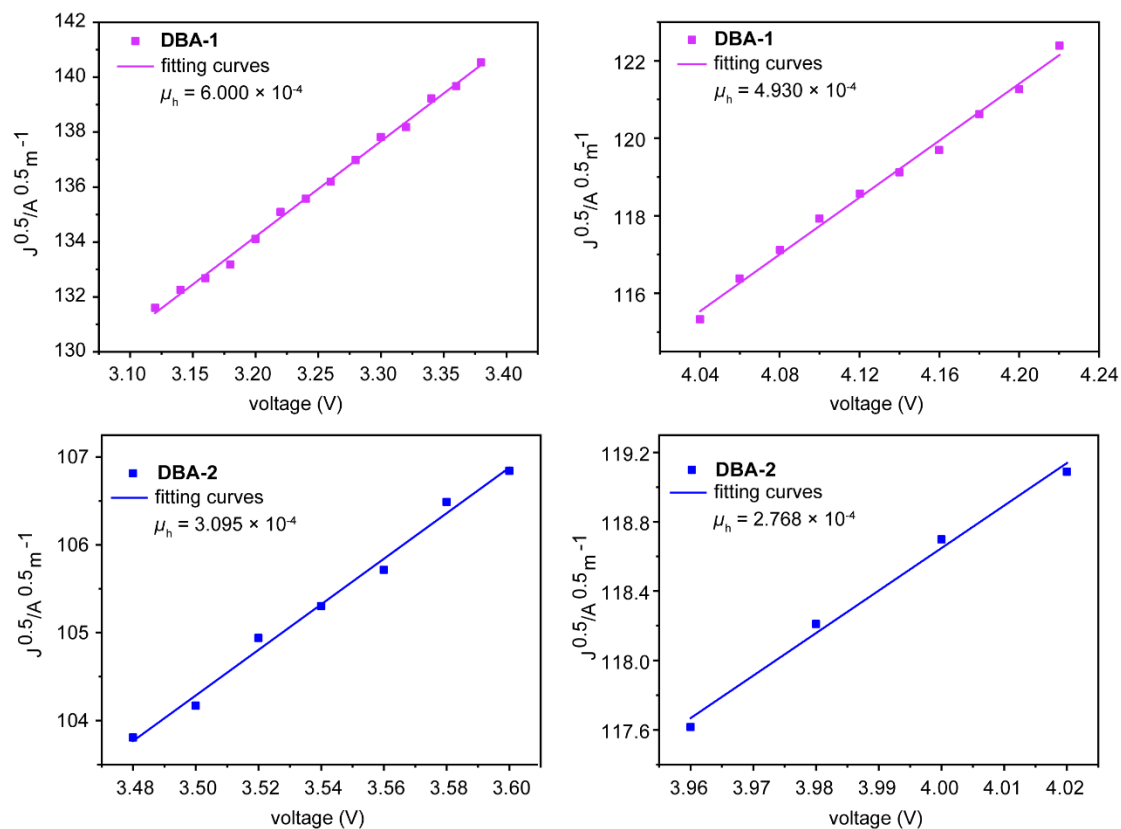


Figure S12.  $J^{0.5}$  vs V plots of hole-only devices of the DBA-1 and DBA-2 films.

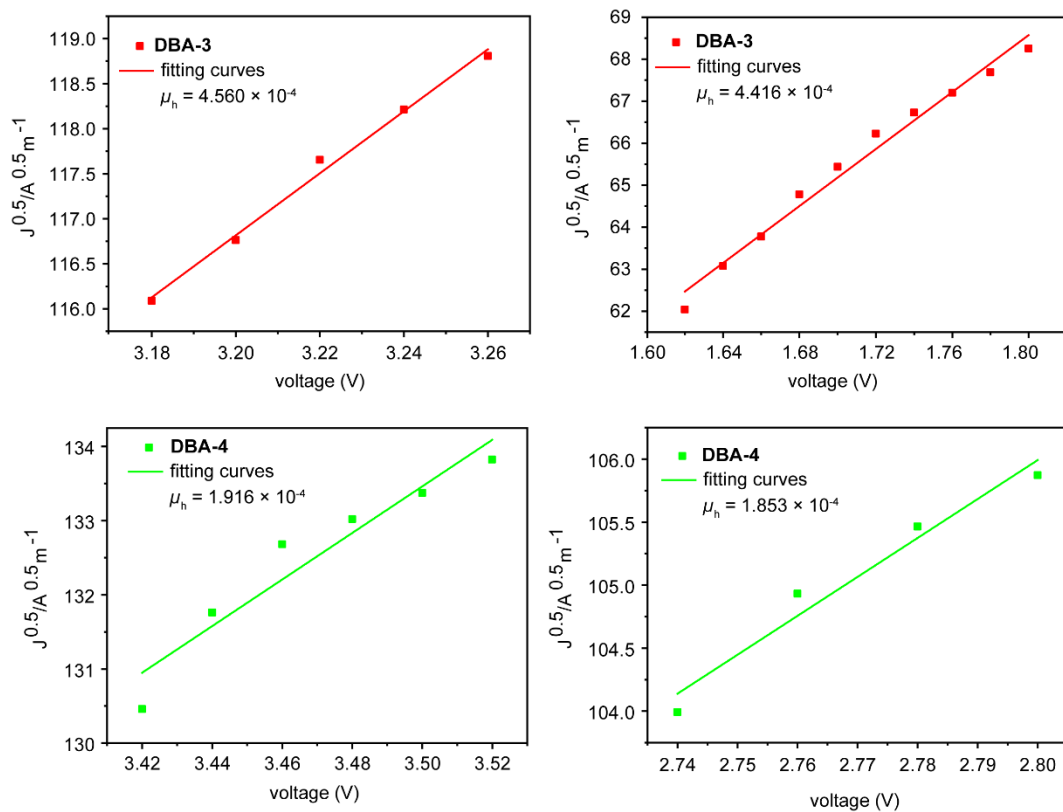
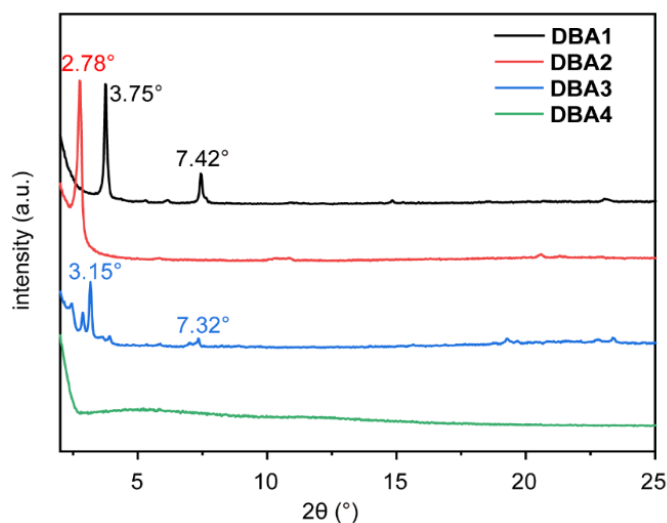


Figure S13.  $J^{0.5}$  vs V plots of hole-only devices of the DBA-3 and DBA-4 films.

## X-ray Diffraction Patterns of Thin Films



**Figure S14.** X-ray diffraction patterns of **DBA-n** films.

The packing pattern of DBA-n molecules in the solid film also plays a critical role in the SCLC charge-carrier mobilities, as revealed by distinct structural characteristics in the X-ray diffraction (XRD) analysis shown above (**Figure S14**), which correlate with their hole mobility trends. For example, **DBA-1** exhibits a sharp, intense peak at  $3.75^\circ$  and a minor peak at  $7.42^\circ$ , indicating a highly ordered crystalline structure with large  $d$ -spacing, consistent with its highest hole mobility among the measured samples. **DBA-2** shows a single intense peak at a lower angle ( $2.78^\circ$ ) but lacks higher-order peaks, suggesting expanded interlayer spacing yet reduced long-range ordering, which aligns with its decreased hole mobility compared to **DBA-1**. In contrast, **DBA-3** displays a triplet peak near  $3.15^\circ$  and a weak peak at  $7.32^\circ$ , which implies slight structural heterogeneity, coinciding with its partial recovery in hole mobility. **DBA-4**, exhibiting no detectable peaks, is likely amorphous or nanocrystalline, corresponding to its lowest hole mobility. These results demonstrate that while larger  $d$ -spacing (**DBA-2**) may degrade charge transport, optimal crystallinity (**DBA-1**) enhances mobility, whereas structural disorder (**DBA-3**) introduces intermediate performance, and amorphousness (**DBA-4**) severely limits conduction. The interplay between crystalline ordering, interlayer spacing, and defect states thus also governs the hole transport properties in these films.

## Thermal Analysis

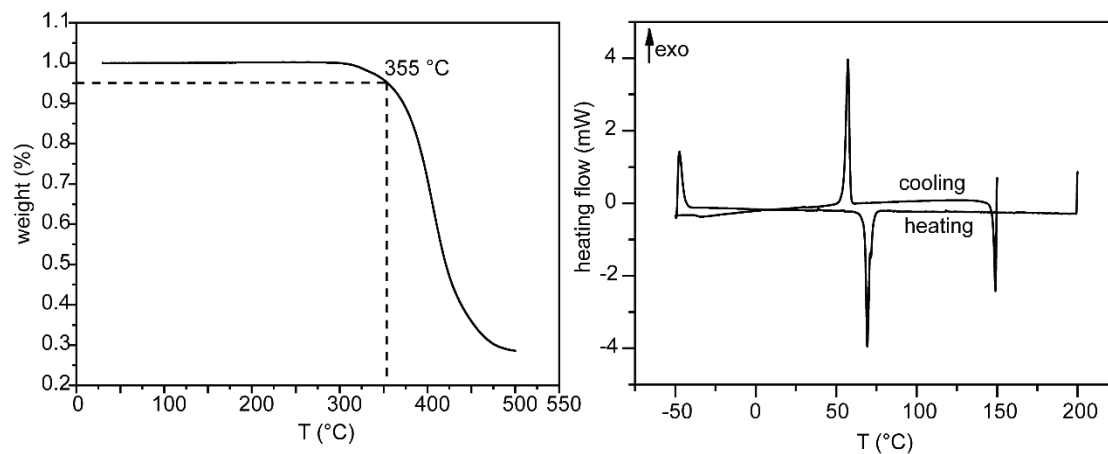


Figure S15. TGA (left) and DSC (right) graph of DBA-1.

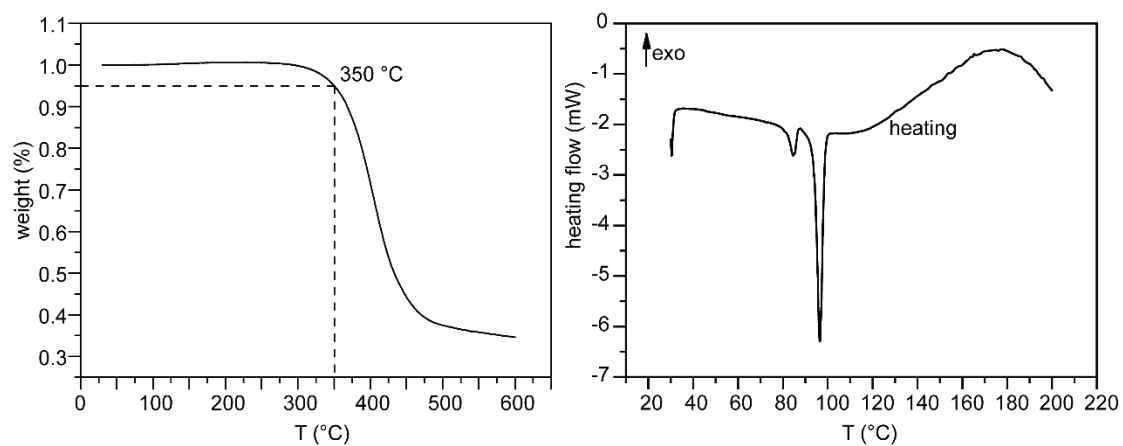


Figure S16. TGA (left) and DSC (right) graph of DBA-2.

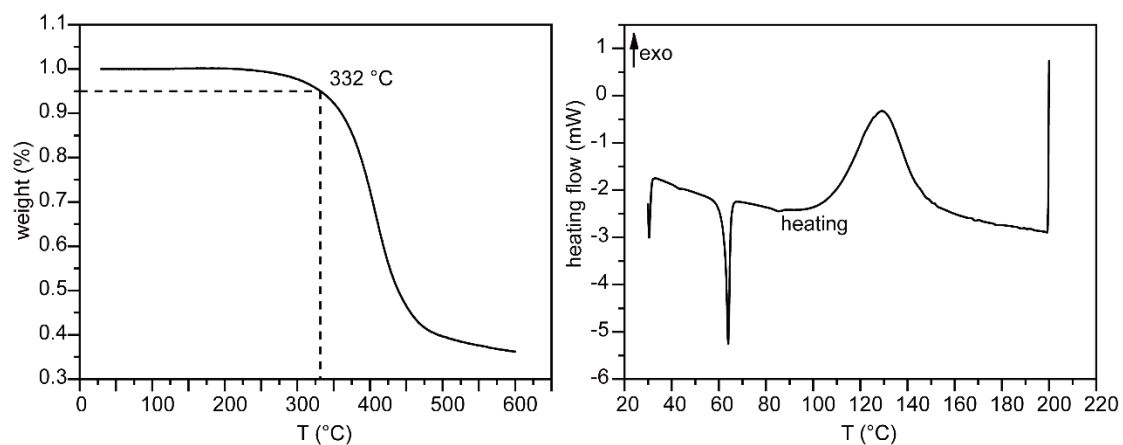
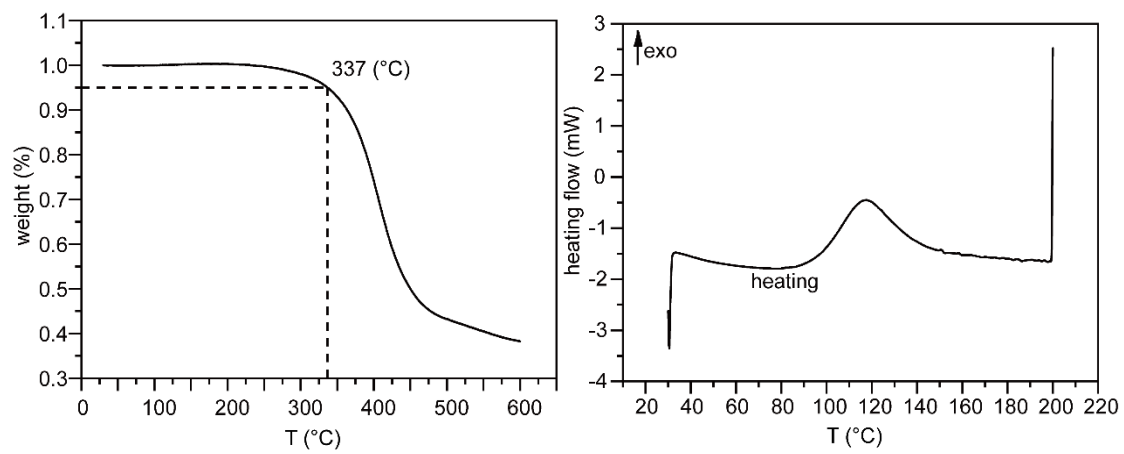
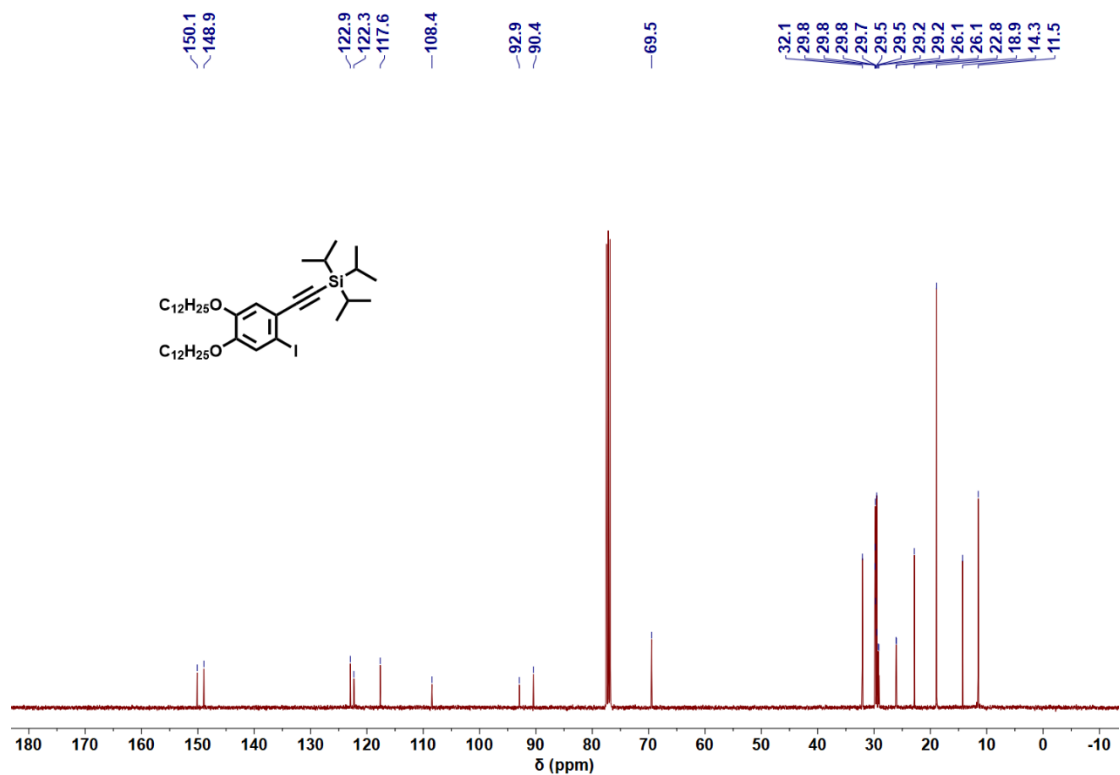
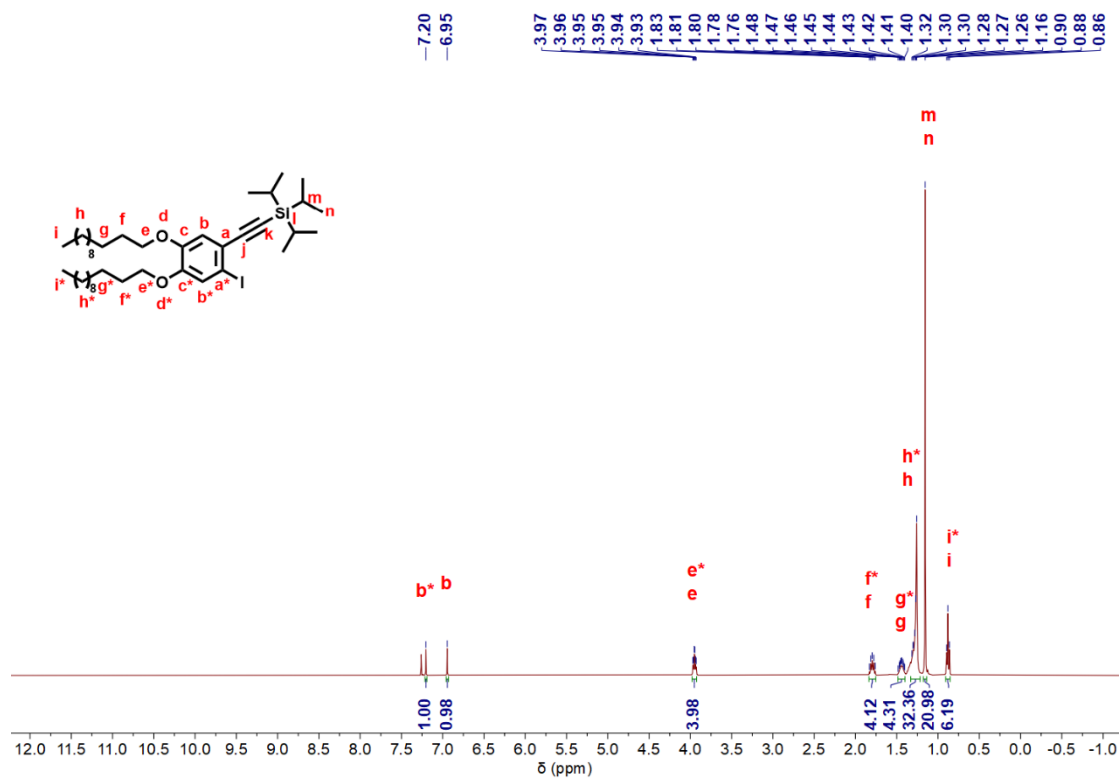


Figure S17. TGA (left) and DSC (right) graph of DBA-3.



**Figure S18.** TGA (left) and DSC (right) graph of **DBA-4**.

# NMR Spectra



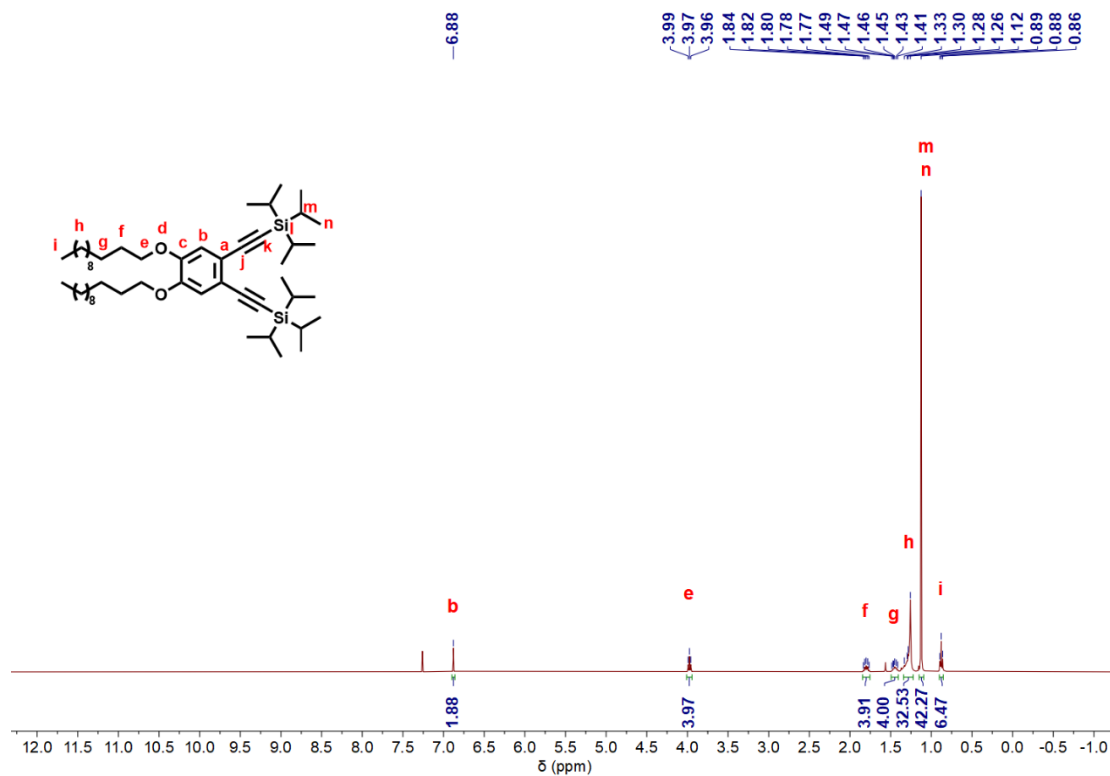


Figure S21. <sup>1</sup>H NMR spectrum of compound 2 in CDCl<sub>3</sub> (400 MHz, 298 K).

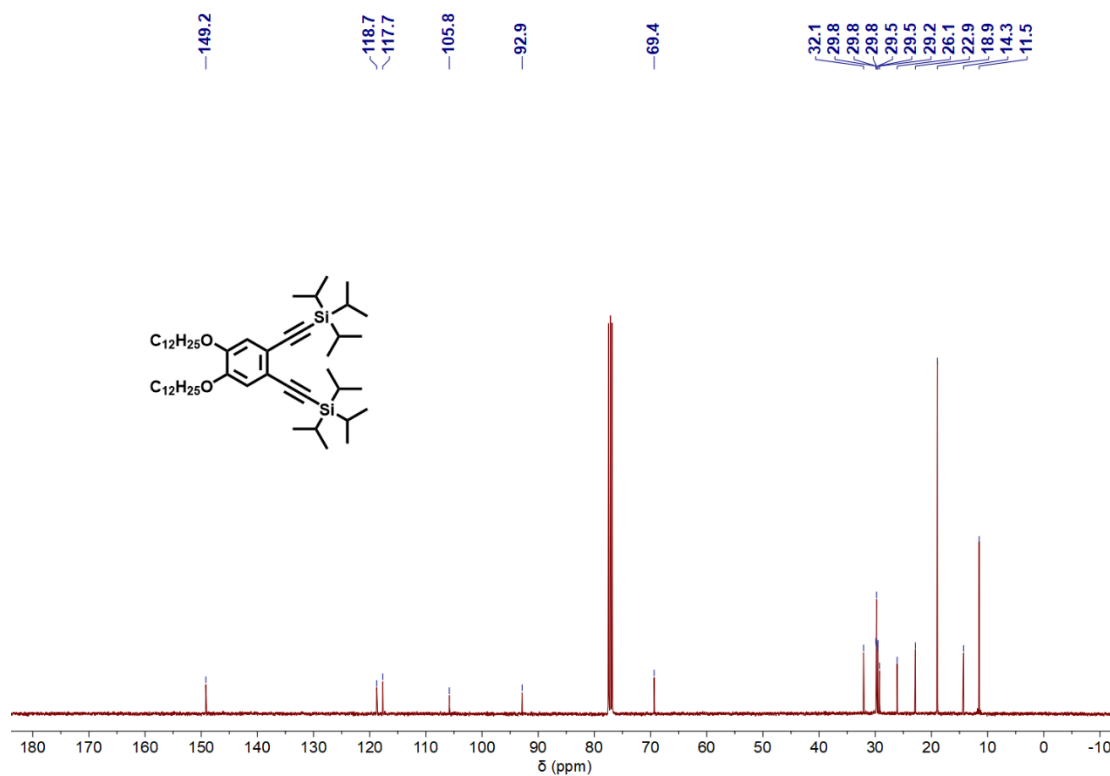
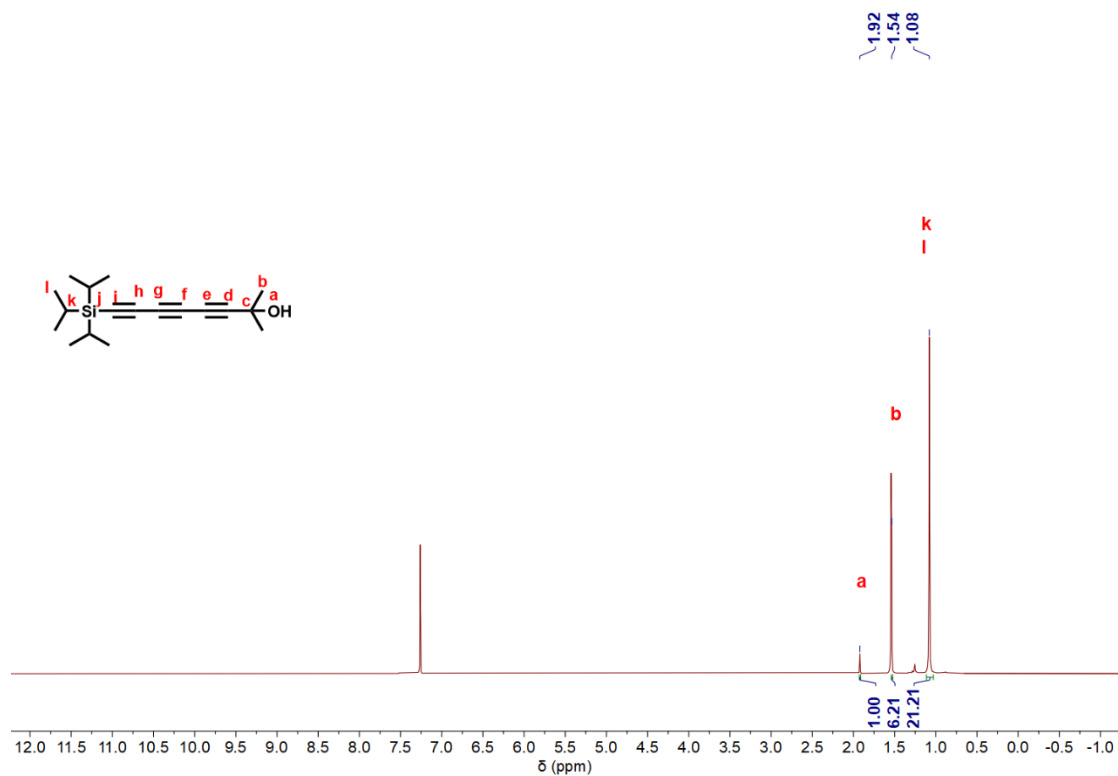
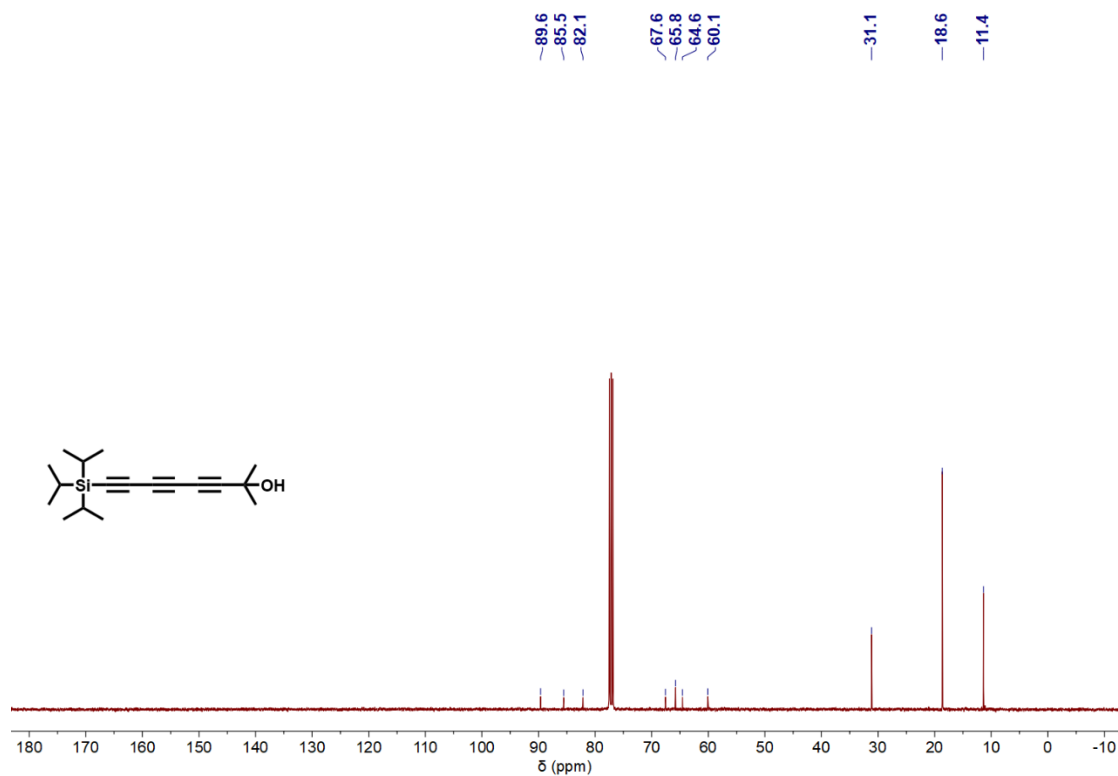


Figure S22. <sup>13</sup>C NMR spectrum of compound 2 in CDCl<sub>3</sub> (101 MHz, 298 K).



**Figure S23.** <sup>1</sup>H NMR spectrum of compound **10** in CDCl<sub>3</sub> (400 MHz, 298 K).



**Figure S24.** <sup>13</sup>C NMR spectrum of compound **10** in CDCl<sub>3</sub> (101 MHz, 298 K).



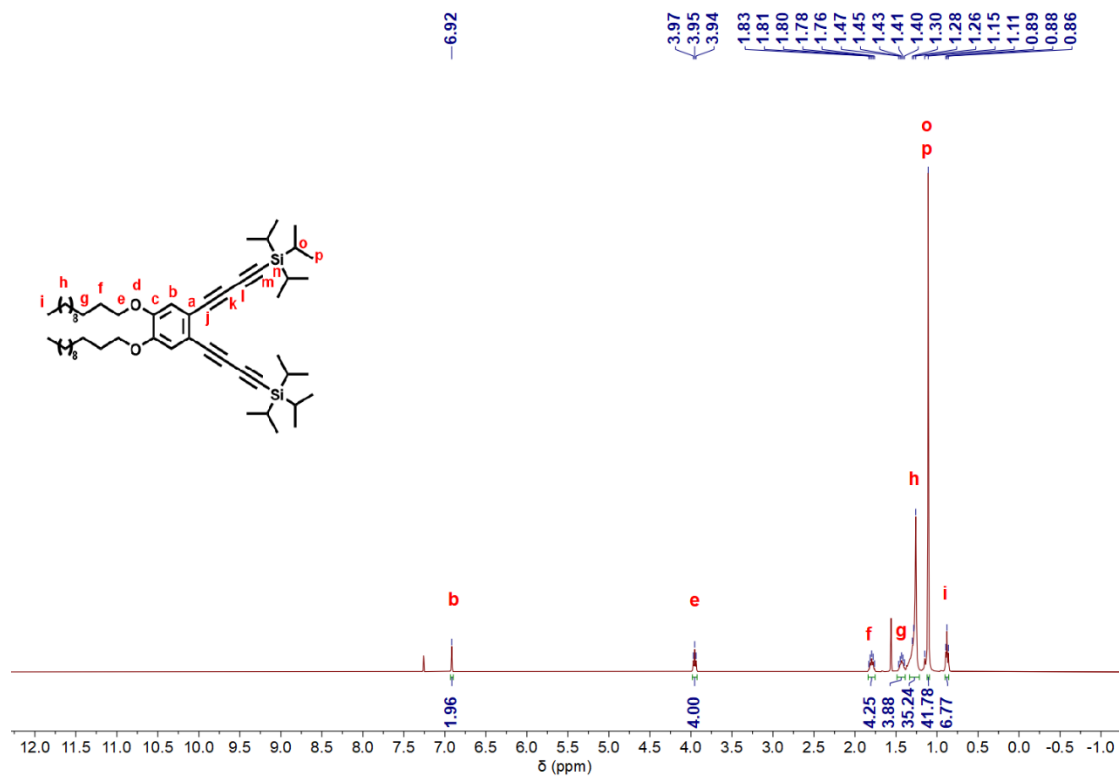


Figure S27.  $^1\text{H}$  NMR spectrum of compound 4 in  $\text{CDCl}_3$  (400 MHz, 298 K).

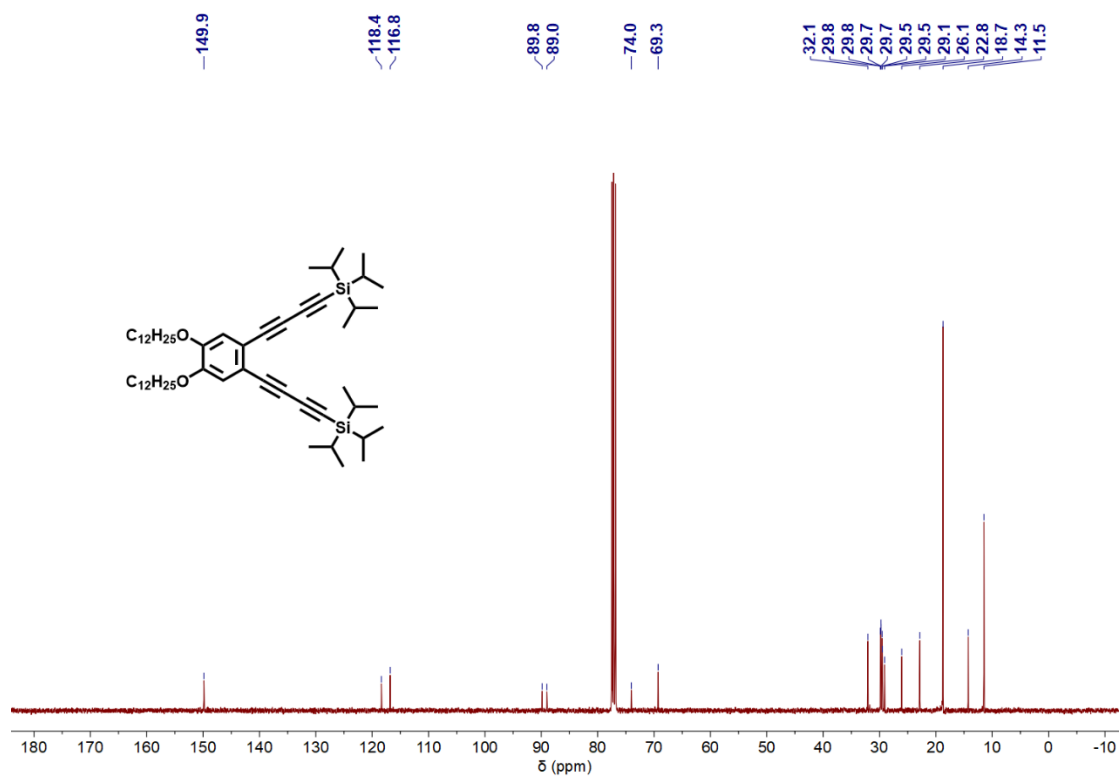


Figure S28.  $^{13}\text{C}$  NMR spectrum of compound 4 in  $\text{CDCl}_3$  (101 MHz, 298 K).

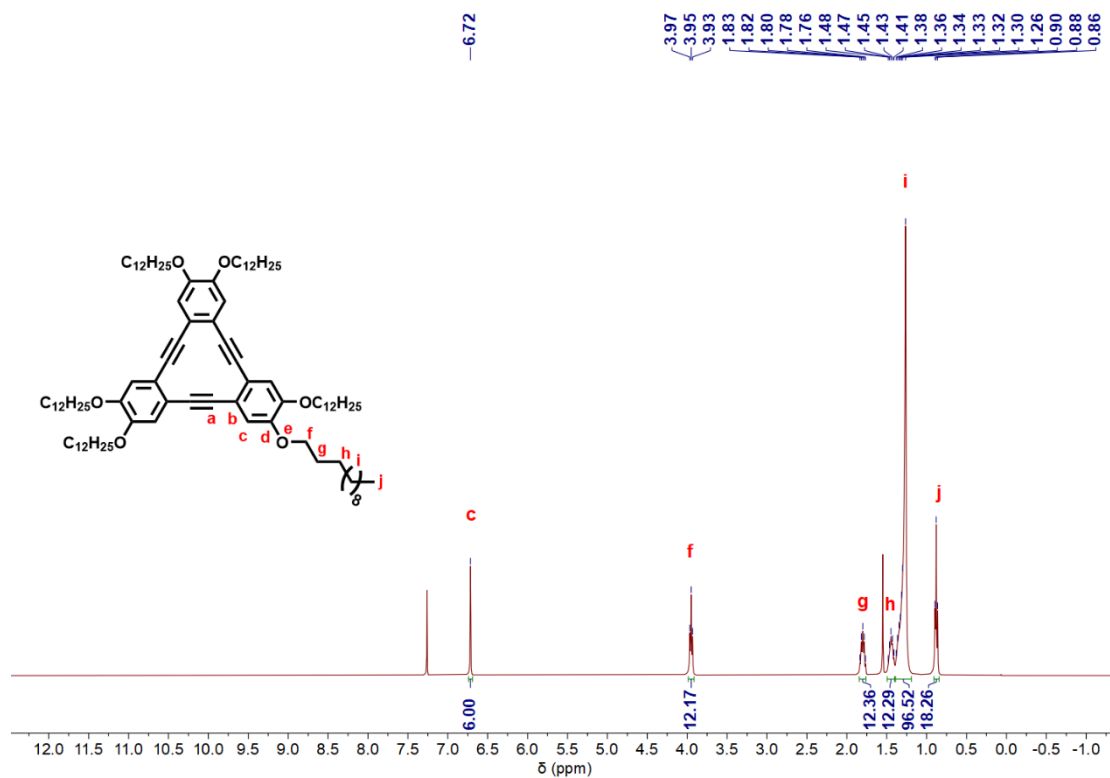


Figure S29.  $^1\text{H}$  NMR spectrum of compound **DBA-1** in  $\text{CDCl}_3$  (400 MHz, 298 K).

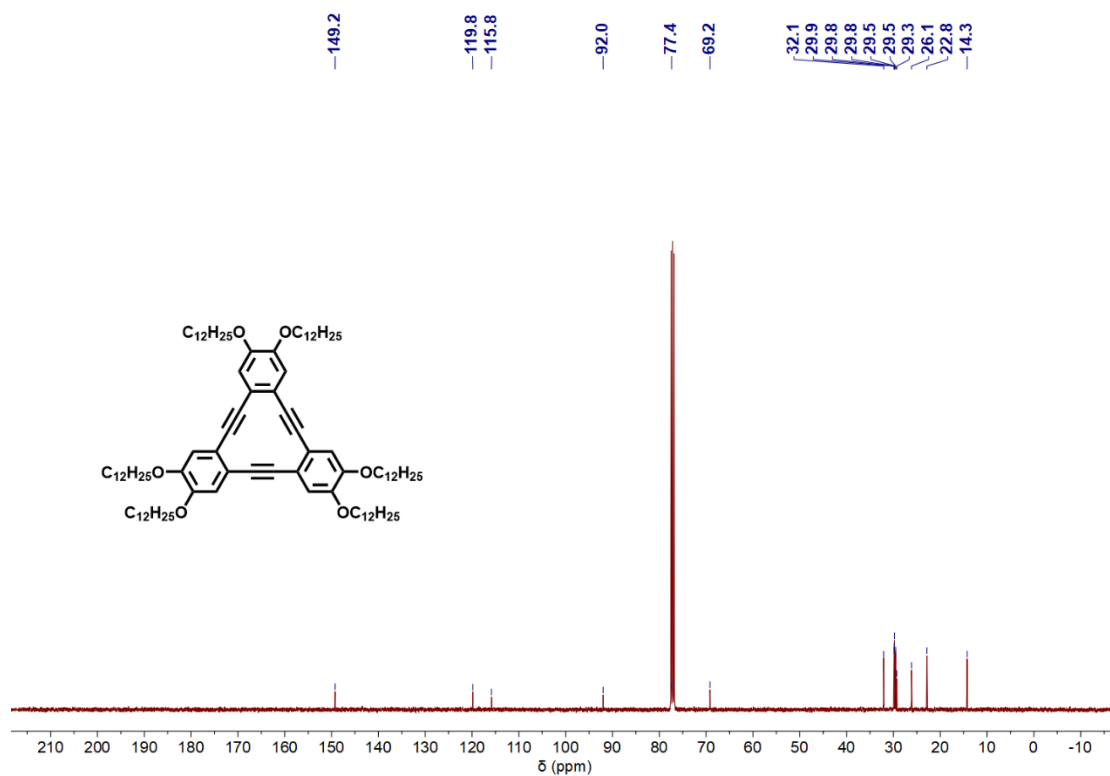


Figure S30.  $^{13}\text{C}$  NMR spectrum of compound **DBA-1** in  $\text{CDCl}_3$  (101 MHz, 298 K).

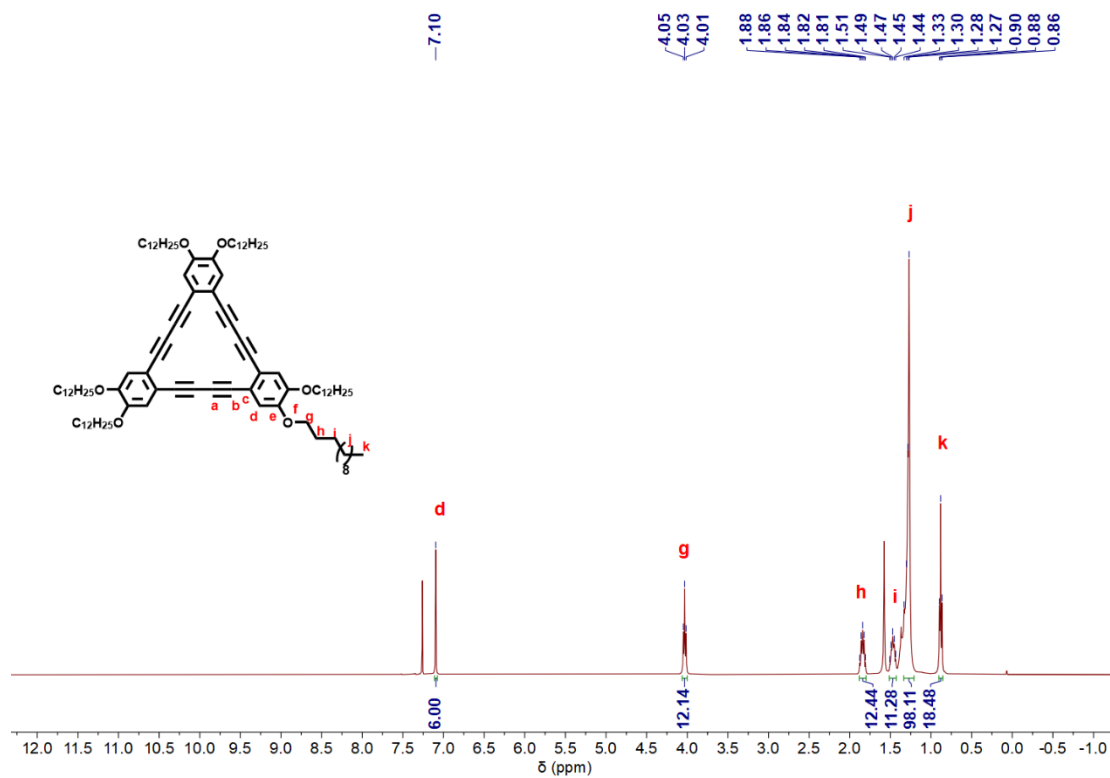


Figure S31. <sup>1</sup>H NMR spectrum of compound **DBA-2** in CDCl<sub>3</sub> (400 MHz, 298 K).

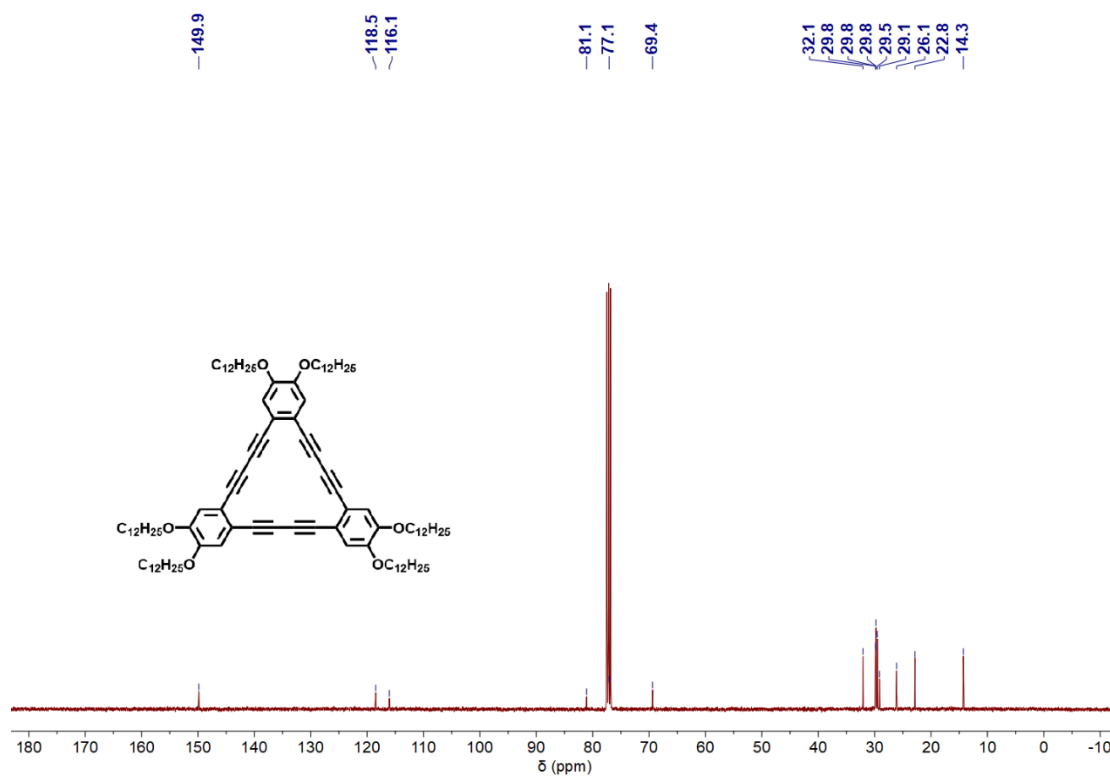
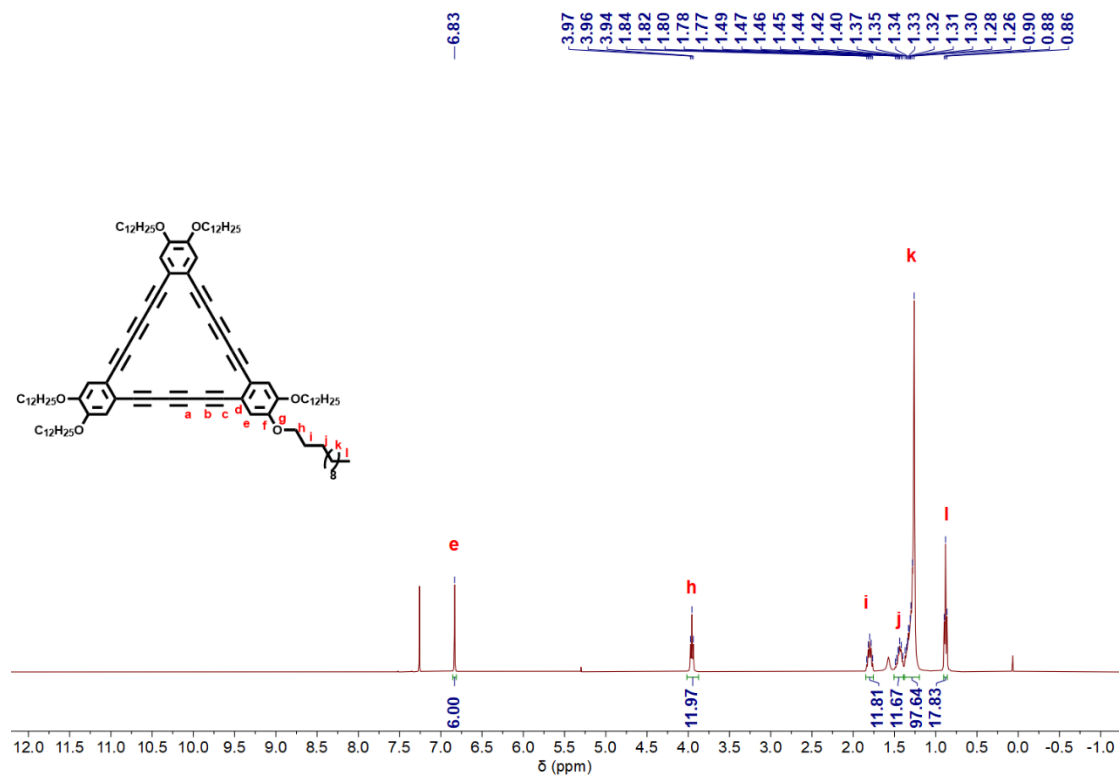
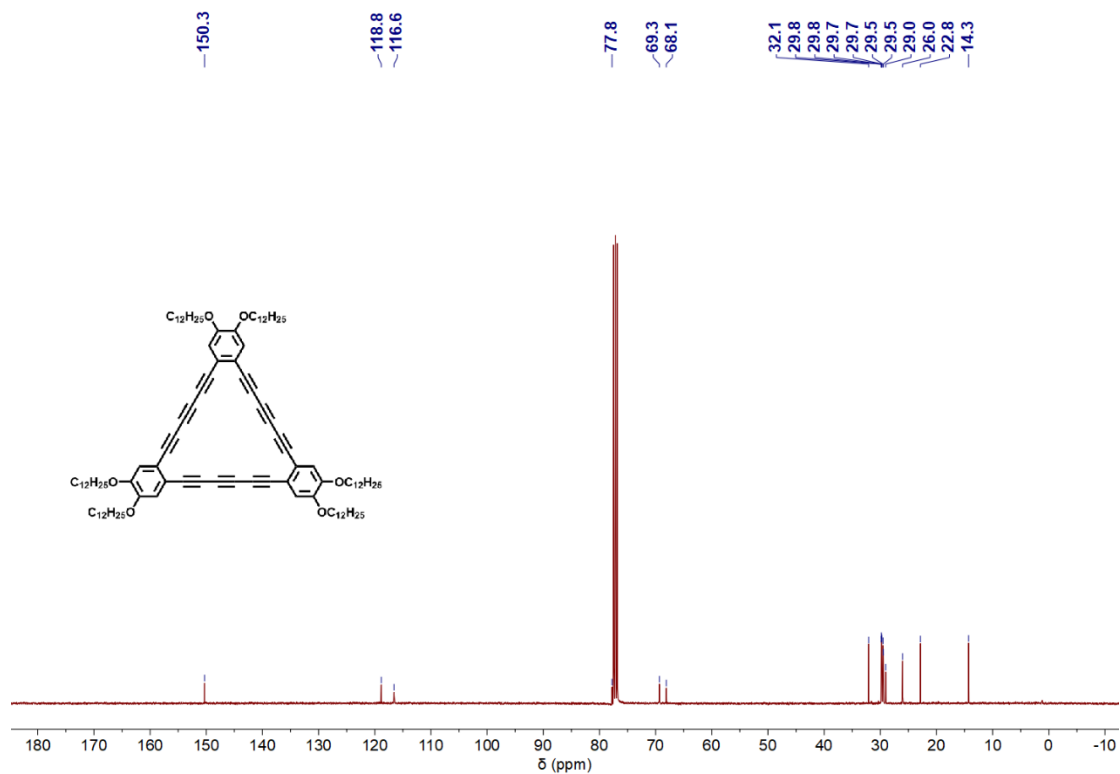


Figure S32. <sup>13</sup>C NMR spectrum of compound **DBA-2** in CDCl<sub>3</sub> (101 MHz, 298 K).



**Figure S33.**  $^1\text{H}$  NMR spectrum of compound **DBA-3** in  $\text{CDCl}_3$  (400 MHz, 298 K).



**Figure 34.**  $^{13}\text{C}$  NMR spectrum of compound **DBA-3** in  $\text{CDCl}_3$  (101 MHz, 298 K).

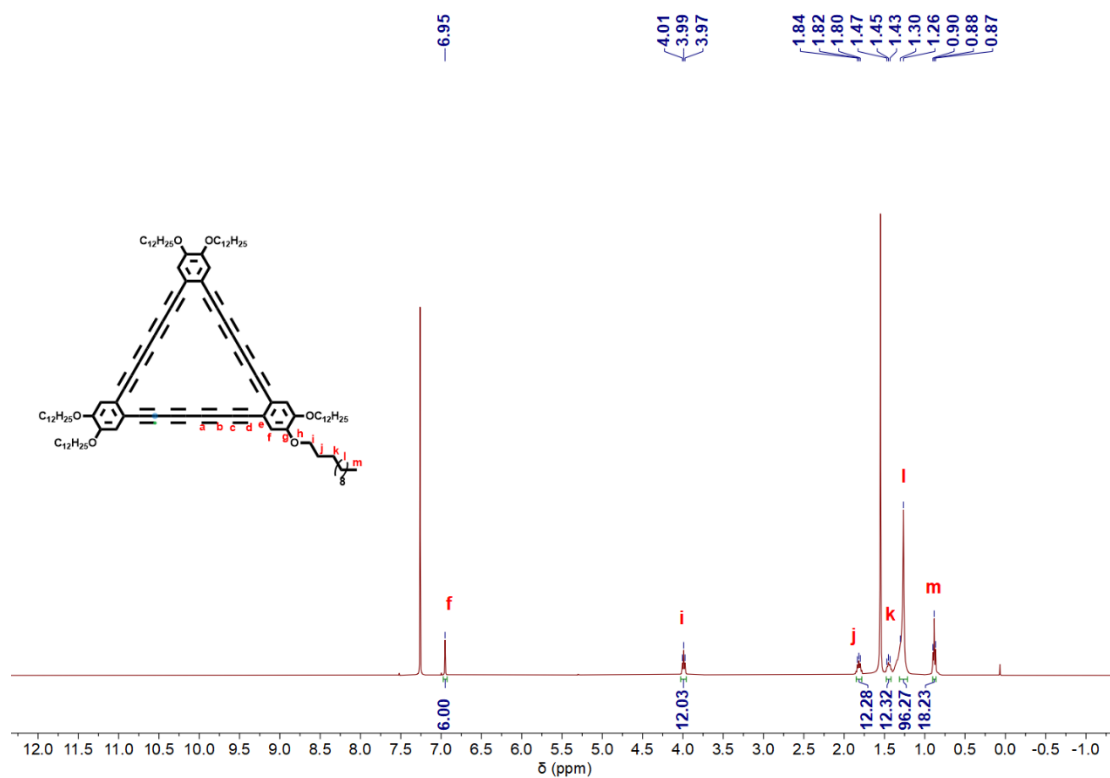


Figure S35. <sup>1</sup>H NMR spectrum of compound **DBA-4** in CDCl<sub>3</sub> (400 MHz, 298 K).

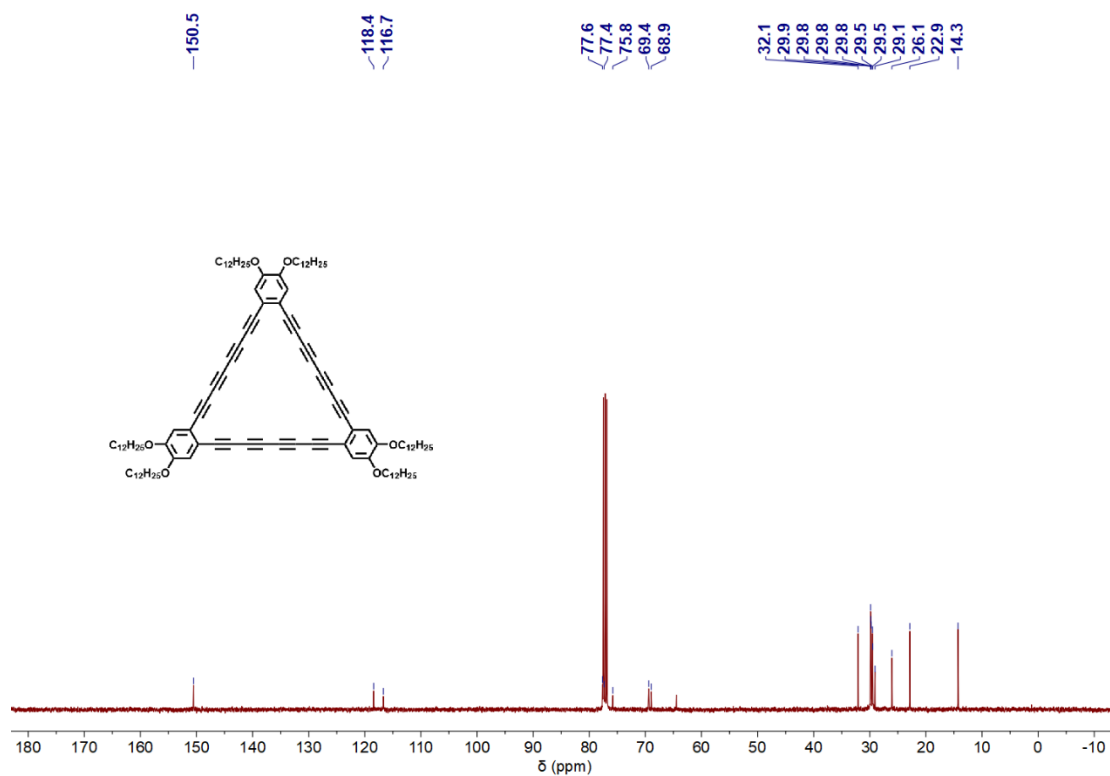
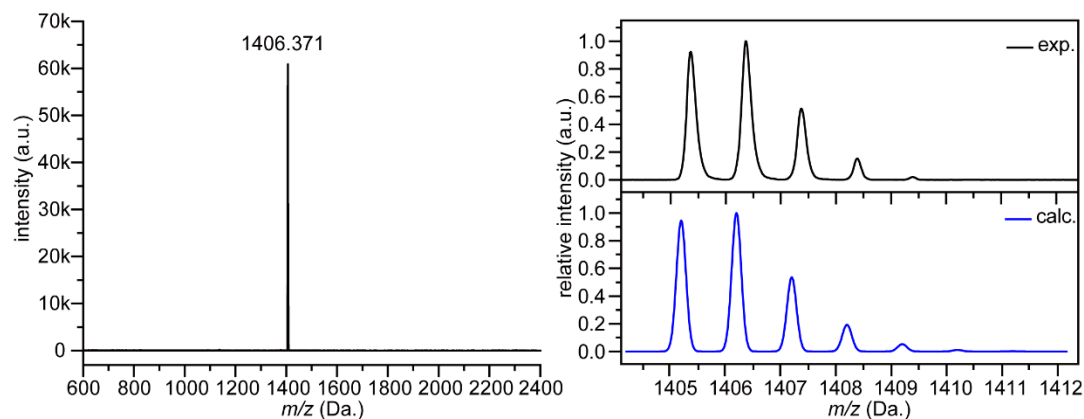
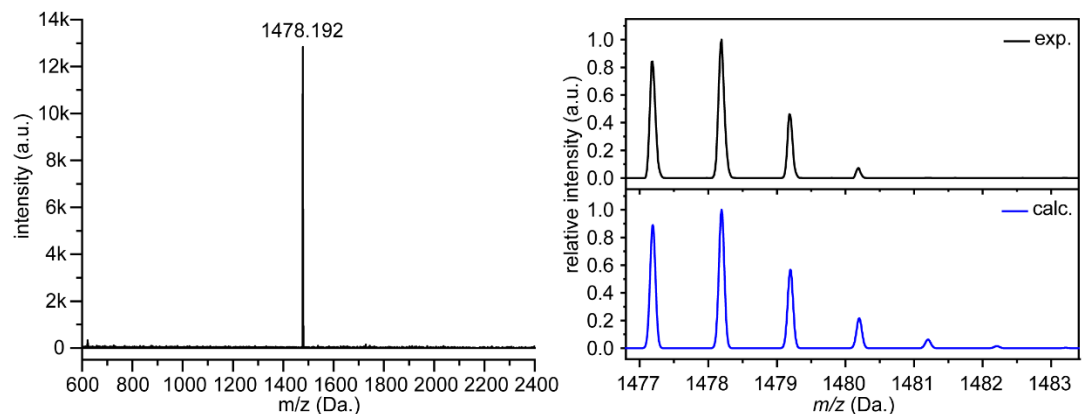


Figure S36. <sup>13</sup>C NMR spectrum of compound **DBA-4** in CDCl<sub>3</sub> (101 MHz, 298 K).

## MALDI-TOF MS Spectra



**Figure S37.** MALDI-TOF MS (DCTB in  $\text{CHCl}_3$  as matrix) spectrum of compound **DBA-1**, right: comparison of experimental isotopic distribution pattern with simulation.



**Figure S38.** MALDI-TOF MS (DCTB in  $\text{CHCl}_3$  as matrix) spectrum of compound **DBA-2**, right: comparison of experimental isotopic distribution pattern with simulation.

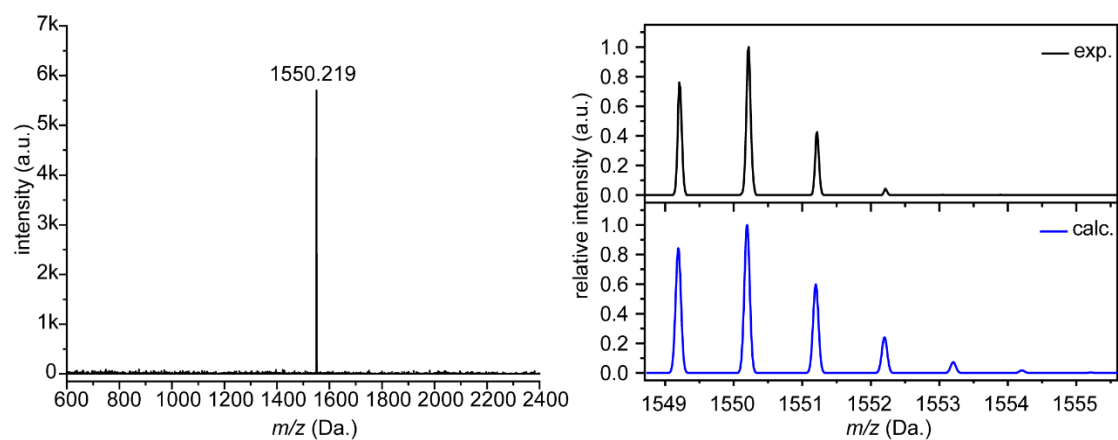


**Figure S39.** MALDI-TOF MS (DCTB in  $\text{CHCl}_3$  as matrix) spectrum of compound **DBA-3**, right: comparison of experimental isotopic distribution pattern with simulation.

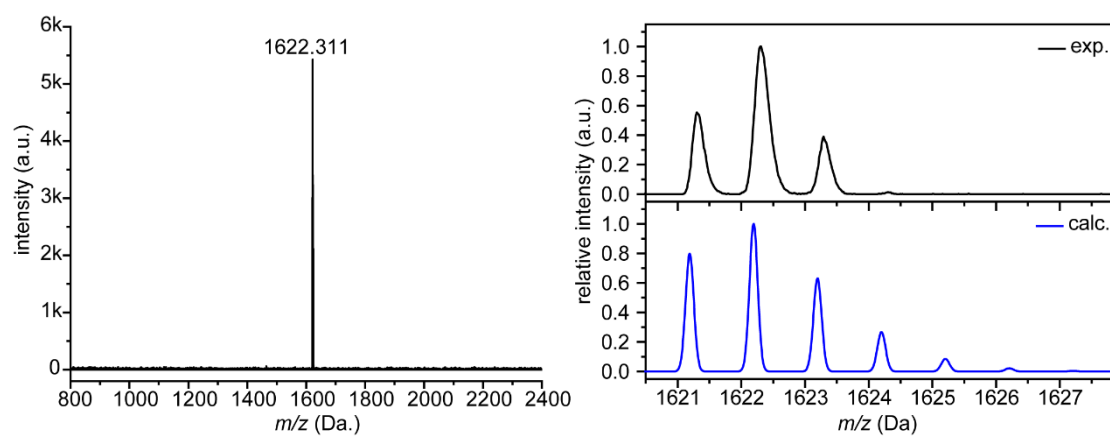


**Figure S40.** MALDI-TOF MS (DCTB in  $\text{CHCl}_3$  as matrix) spectrum of compound **DBA-4**, right: comparison of experimental isotopic distribution pattern with simulation.

## References

1. Gaussian 09, Revision D.01, G. W. T. M. J. Frisch, H. B. Schlegel, G. E. Scuseria, M. A. Robb, J. R. Cheeseman, G. Scalmani, V. Barone, B. Mennucci, G. A. Petersson, H. Nakatsuji, M. Caricato, X. Li, H. P. Hratchian, A. F. Izmaylov, J. Bloino, G. Zheng, J. L. Sonnenberg, M. Hada, M. Ehara, K. Toyota, R. Fukuda, J. Hasegawa, M. Ishida, T. Nakajima, Y. Honda, O. Kitao, H. Nakai, T. Vreven, J. A. Montgomery, Jr., J. E. Peralta, F. Ogliaro, M. Bearpark, J. J. Heyd, E. Brothers, K. N. Kudin, V. N. Staroverov, T. Keith, R. Kobayashi, J. Normand, K. Raghavachari, A. Rendell, J. C. Burant, S. S. Iyengar, J. Tomasi, M. Cossi, N. Rega, J. M. Millam, M. Klene, J. E. Knox, J. B. Cross, V. Bakken, C. Adamo, J. Jaramillo, R. Gomperts, R. E. Stratmann, O. Yazyev, A. J. Austin, R. Cammi, C. Pomelli, J. W. Ochterski, R. L. Martin, K. Morokuma, V. G. Zakrzewski, G. A. Voth, P. Salvador, J. J. Dannenberg, S. Dapprich, A. D. Daniels, O. Farkas, J. B. Foresman, J. V. Ortiz, J. Cioslowski, and D. J. Fox, Gaussian, Inc., Wallingford CT, 2013.
2. A. D. Becke, *J. Chem. Phys.*, 1993, **98**, 5648-5652.
3. P. J. Stephens, F. J. Devlin, C. F. Chabalowski and M. J. Frisch, *J. Phys. Chem.*, 2002, **98**, 11623-11627.
4. Z. Chen, C. S. Wannere, C. Corminboeuf, R. Puchta and P. v. R. Schleyer, *Chem. Rev.*, 2005, **105**, 3842-3888.
5. H. Fallah-Bagher-Shaidaei, C. S. Wannere, C. Corminboeuf, R. Puchta and P. v. R. Schleyer, *Org. Lett.*, 2006, **8**, 863-866.
6. K. Tahara, S. Furukawa, H. Uji-i, T. Uchino, T. Ichikawa, J. Zhang, W. Mamdouh, M. Sonoda, F. C. De Schryver, S. De Feyter and Y. Tobe, *J. Am. Chem. Soc.*, 2006, **128**, 16613-16625.
7. A. S. Dillon and B. L. Flynn, *Org. Lett.*, 2020, **22**, 2987-2990.
8. K. Tahara, C. A. Johnson, T. Fujita, M. Sonoda, F. C. De Schryver, S. De Feyter, M. M. Haley and Y. Tobe, *Langmuir*, 2007, **23**, 10190-10197.

## Calculated Molecular Cartesian Coordinates

### DBA-1'

E(RB3LYP) = -1608.789547 a.u.

Charge = 0; Multiplicity = 1

	x	y	z				
				O	6.473264	-1.02615	0.000057
C	-3.55297	-3.85865	0.000058	C	7.025286	0.280717	0.000035
C	-4.45783	-2.76376	-4E-06	O	0.208383	6.550593	0.000107
C	-3.95977	-1.46691	-0.00011	O	-2.34756	6.119083	0.000015
C	-2.57285	-1.2082	-0.00016	C	-3.75537	5.943952	0.000541
C	-1.67	-2.3006	-0.0001	C	1.595733	6.847224	0.000207
C	-2.18542	-3.61392	0.000004	H	-4.63528	-0.62141	-0.00015
C	-2.09928	0.132222	-0.00029	H	-1.48226	-4.4366	0.000037
C	-0.26438	-2.08773	-0.00016	H	-3.101	3.501007	-0.00021
C	-1.6753	1.272495	-0.00033	H	1.779412	4.325508	-2.9E-05
C	0.935164	-1.88511	-0.00018	H	4.582462	0.934752	-0.00009
C	-1.15704	2.596295	-0.0002	H	2.856399	-3.70388	-2.4E-05
C	2.33274	-1.62468	-0.00011	H	-7.7068	-2.5218	-0.00016
C	-2.03706	3.699021	-0.00014	H	-6.63385	-1.41082	0.893662
C	-1.56554	5.005808	-2.8E-05	H	-6.6337	-1.41102	-0.89406
C	-0.16493	5.242256	0.000007	H	-3.92777	-7.09497	0.000536
C	0.709552	4.162799	-6.1E-05	H	-2.63459	-6.25063	-0.89349
C	0.240457	2.83225	-0.00015	H	-2.63458	-6.25028	0.894226
C	2.826984	-0.29643	-0.00013	H	6.039598	-5.41221	0.000368
C	4.221989	-0.08564	-7.6E-05	H	4.540684	-5.03937	0.894057
C	5.118111	-1.14713	0.000001	H	4.540787	-5.03959	-0.89358
C	4.62279	-2.47842	0.000026	H	8.107879	0.147463	0.000087
C	3.250704	-2.69606	-3.4E-05	H	6.729886	0.84498	-0.89384
C	1.164638	1.752015	-0.0002	H	6.729809	0.845042	0.893844
C	1.939757	0.81436	-0.0002	H	-4.18111	6.948194	0.000924
O	-4.12637	-5.09249	0.000155	H	-4.09622	5.405822	0.894364
O	-5.77763	-3.09425	0.000061	H	-4.09695	5.406216	-0.89324
C	-6.72781	-2.04082	-0.00014	H	1.668321	7.935568	0.000336
C	-3.27092	-6.22416	0.000367	H	2.094446	6.450923	0.894013
O	5.569435	-3.45558	0.0001	H	2.094529	6.451132	-0.89365
C	5.133158	-4.80548	0.000242				

### DBA-2'

E(RB3LYP) = -1837.270768 a.u.

Charge = 0; Multiplicity = 1

	x	y	z				
				C	3.352549	-0.05565	-8.7E-05
C	6.374847	2.122378	0.000065	C	0.941433	2.706861	-4.1E-05
C	5.784634	3.419186	0.000062	C	2.658857	-1.06325	-0.00012
C	4.403361	3.540941	0.000029	C	-0.40819	2.836386	0.000014
C	3.56112	2.404906	-8E-06	C	1.871763	-2.16721	-0.00012
C	4.149591	1.111964	-1.9E-05	C	-1.62762	2.933703	0.000024
C	5.559404	1.000888	0.00002	C	1.145586	-3.15165	-0.00011
C	2.157095	2.570329	-3.3E-05	C	-3.03742	3.039181	0.000002

C	0.301188	-4.28551	-5.7E-05	C	-4.91994	6.838252	-0.00076
C	-3.64747	4.315071	-9.5E-05	H	3.938186	4.517837	0.000035
C	-5.02662	4.458838	-9.9E-05	H	5.990545	0.008497	0.000004
C	-5.85339	3.298467	0.000048	H	-3.00473	5.185549	-0.00016
C	-5.26689	2.042018	0.00013	H	-5.87942	1.150034	0.000204
C	-3.86175	1.882286	0.000118	H	-2.98851	-5.19377	0.000105
C	-1.1129	-4.14976	0.00004	H	1.943737	-5.66768	-0.00012
C	-1.91332	-5.31563	0.000067	H	9.449989	1.051508	0.000455
C	-1.34868	-6.58206	0.000024	H	8.126604	0.254513	0.894328
C	0.069595	-6.71822	-9.1E-05	H	8.126901	0.254396	-0.89375
C	0.865034	-5.58247	-9.5E-05	H	6.99721	6.441256	0.000194
C	-3.30199	0.584123	0.000197	H	5.527023	5.96722	-0.89388
C	-1.72602	-2.87593	0.000096	H	5.52696	5.967146	0.89413
C	-2.81345	-0.53738	0.000226	H	2.082172	-9.27788	-0.00129
C	-2.25132	-1.77117	0.000133	H	2.405044	-7.76702	-0.89491
O	6.660691	4.456721	0.000102	H	2.405865	-7.7677	0.893152
O	7.732631	2.101436	0.000104	H	-3.84145	-7.16761	0.894689
C	8.380621	0.837732	0.000294	H	-3.84214	-7.16783	-0.89338
C	6.133558	5.775423	0.000137	H	-3.81146	-8.7121	0.000827
O	0.530807	-7.99535	-0.00011	H	-9.07631	2.834261	0.000493
O	-2.04459	-7.74806	0.000048	H	-7.92982	1.799133	-0.89362
C	1.93651	-8.19713	-0.00083	H	-7.9295	1.799387	0.894501
C	-3.46297	-7.67876	0.000571	H	-5.64079	7.656547	-0.00109
O	-7.1902	3.537008	0.000062	H	-4.28802	6.910377	-0.89483
C	-8.06743	2.420248	0.000376	H	-4.28797	6.911169	0.893221
O	-5.68888	5.644279	-0.0002				

### DBA-3'

E(RB3LYP) = -2065.750837 a.u.

Charge = 0; Multiplicity = 1

	x	y	z				
C	1.077067	8.12889	-0.00004	C	-5.40849	-2.00817	0.000041
C	-0.34599	8.192389	0.000009	C	5.206084	-2.48463	-4.1E-05
C	-1.08273	7.016429	0.00005	C	-6.82099	-1.96806	-0.00012
C	-0.4525	5.751702	0.00004	C	-7.57838	-3.13079	-0.00018
C	0.965849	5.6884	-2E-06	C	-6.92255	-4.39529	-9.5E-05
C	1.706185	6.892005	-0.00004	C	-5.53579	-4.44613	0.000063
C	-1.23773	4.575146	0.000093	C	-4.75482	-3.26848	0.000127
C	1.643076	4.446524	0.000027	C	4.443325	-3.68205	0.000098
C	-1.9224	3.560007	0.000133	C	5.116897	-4.92426	0.000148
C	2.233871	3.374035	0.000062	C	6.502708	-4.99657	-8E-06
C	-2.6635	2.430535	0.000159	C	7.267996	-3.79511	-0.00019
C	2.869967	2.182263	0.000046	C	6.616574	-2.56989	-0.00021
C	-3.32532	1.394635	0.000156	C	-3.34332	-3.36114	0.000268
C	3.435524	1.090818	0.000043	C	3.02917	-3.64909	0.000212
C	-4.03861	0.247394	0.000135	C	-2.12191	-3.44739	0.000352
C	4.042591	-0.116	0.000016	C	1.804956	-3.62498	0.000275
C	-4.67121	-0.80098	0.000096	C	-0.77323	-3.52496	0.000357
C	4.578829	-1.21678	-1.9E-05	C	0.454776	-3.58072	0.000385
				O	1.712305	9.327443	-0.00008

O	-0.87194	9.442729	0.000012	H	3.537597	8.841957	0.89409
C	3.133346	9.332267	-0.00018	H	3.537472	8.841862	-0.89445
C	-2.28686	9.574044	0.000059	H	-2.48567	10.64616	0.000049
O	8.614027	-3.96323	-0.00035	H	-2.73317	9.12163	-0.8942
O	7.224285	-6.1452	0.000019	H	-2.73311	9.121657	0.894359
C	9.434046	-2.80263	-0.00035	H	10.46228	-3.16551	-0.00033
C	6.519414	-7.37909	0.000109	H	9.264778	-2.19011	-0.89463
O	-7.74319	-5.47541	-0.00017	H	9.264754	-2.1901	0.893927
C	-7.15053	-6.76695	-0.00012	H	7.283073	-8.15741	0.000012
O	-8.93399	-3.17914	-0.00033	H	5.892916	-7.4847	0.89447
C	-9.64803	-1.95057	-0.00034	H	5.892689	-7.4847	-0.89409
H	-2.1643	7.046129	0.000089	H	-7.98021	-7.47448	-0.00022
H	2.786093	6.82539	-6.4E-05	H	-6.53568	-6.92765	-0.89434
H	-7.30253	-0.99915	-0.0002	H	-6.53589	-6.92767	0.89425
H	-5.02131	-5.39794	0.000137	H	-9.42514	-1.35548	-0.89463
H	4.519928	-5.82662	0.000299	H	-10.7044	-2.221	-0.0004
H	7.182054	-1.64749	-0.00035	H	-9.42523	-1.35552	0.893983
H	3.426812	10.38243	-0.00025				

#### DBA-4'

E(RB3LYP) = -2294.233582 a.u.

Charge = 0; Multiplicity = 1

	x	y	z				
C	9.456996	2.055731	-0.00016	C	-7.49256	6.126809	-0.00022
C	9.054153	3.423351	0.000206	C	-7.08699	4.800262	-0.00035
C	7.703088	3.737994	0.000281	C	-5.71806	4.447721	-0.00029
C	6.71146	2.730544	0.000026	C	-2.37398	-6.84468	0.000102
C	7.112881	1.367965	-0.0003	C	-3.32958	-7.8863	0.000405
C	8.492261	1.058959	-0.00036	C	-2.94635	-9.21949	0.000358
C	5.345492	3.091024	0.00016	C	-1.55999	-9.55218	0.000122
C	6.161001	0.324092	-0.00042	C	-0.61356	-8.5379	-0.00022
C	4.163178	3.414115	0.000295	C	-5.3452	3.085096	-0.00043
C	5.345479	-0.59087	-0.00047	C	-2.80359	-5.49886	0.000208
C	2.859087	3.754603	0.000316	C	-5.03392	1.899624	-0.00054
C	4.437453	-1.5869	-0.0005	C	-3.18661	-4.33459	0.00017
C	1.663592	4.053204	0.000342	C	-4.67717	0.599884	-0.0003
C	3.598599	-2.48949	-0.0005	C	-3.59535	-3.05025	0.000057
C	0.357569	4.365208	0.000228	C	-4.33903	-0.58503	-0.00029
C	2.674344	-3.46355	-0.00054	C	-3.95763	-1.8725	0.000098
C	-0.84367	4.63979	0.000184	O	10.79589	1.845345	-0.00019
C	1.817592	-4.34917	-0.00052	O	10.06545	4.325664	0.000435
C	-2.16028	4.928092	-2.5E-05	C	9.731736	5.707624	0.001158
C	0.871468	-5.30908	-0.00058	C	11.26404	0.503041	-0.00102
C	-3.36018	5.17806	-8.8E-05	O	-7.00103	8.425205	0.00023
C	0.000982	-6.1719	-0.00051	O	-8.78068	6.548308	-0.00026
C	-4.7406	5.478406	-5.6E-05	C	-9.80784	5.565315	-0.00099
C	-0.99263	-7.17613	-0.00014	C	-6.07426	9.503354	0.001485
C	-5.16518	6.826695	0.000074	O	-1.28197	-10.8787	0.000109
C	-6.51147	7.161366	0.00006	C	0.082412	-11.2781	0.00124
				O	-3.796	-10.2754	0.00068

C	-5.19322	-10.0124	-8.7E-05	H	-10.7476	6.118161	-0.00136
H	7.379456	4.770462	0.000533	H	-9.75765	4.932443	-0.89555
H	8.780173	0.015984	-0.00054	H	-9.75858	4.932072	0.893354
H	-4.40714	7.598664	0.000168	H	-6.67638	10.4123	0.002248
H	-7.81781	4.002484	-0.00049	H	-5.43925	9.488283	-0.89281
H	-4.37722	-7.6162	0.000711	H	-5.43964	9.486494	0.896022
H	0.442791	-8.77192	-0.00057	H	0.072336	-12.3683	0.0024
H	10.68194	6.242294	0.001519	H	0.60684	-10.9202	-0.89331
H	9.159581	5.983208	-0.8932	H	0.605907	-10.9182	0.895541
H	9.159439	5.982229	0.895724	H	-5.49772	-9.45509	0.894327
H	12.35237	0.568456	-0.00137	H	-5.49665	-9.45464	-0.89458
H	10.93249	-0.03862	0.893356	H	-5.67885	-10.9885	-0.00061
H	10.93184	-0.03775	-0.89567				